Appendix.

A chemical-genetic interaction map of small molecules using high-throughput imaging in cancer cells

Breinig et al.

Table of content:

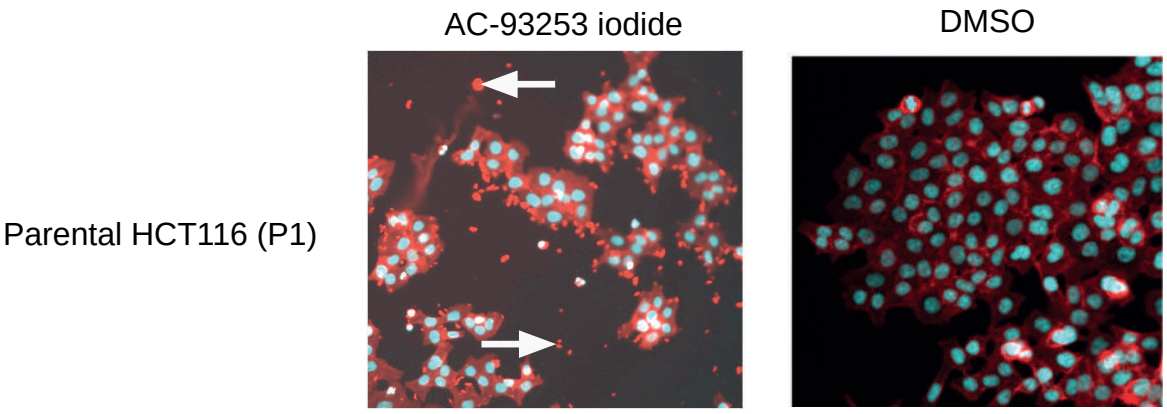

Appendix Figure S1. Quality control.
Images showing experimental artefact, such as autofluorescence of AC-93253 iodide, were removed from the analysis.
Here, a high fluorescence background and the occurence of fluorescent speckles (arrows) can be seen in the TRITC channel used to detect actin via Phalloidin-TRITC staining.
Image of DMSO treated cells is included as a reference, showing low fluorescence background and specific actin staining.

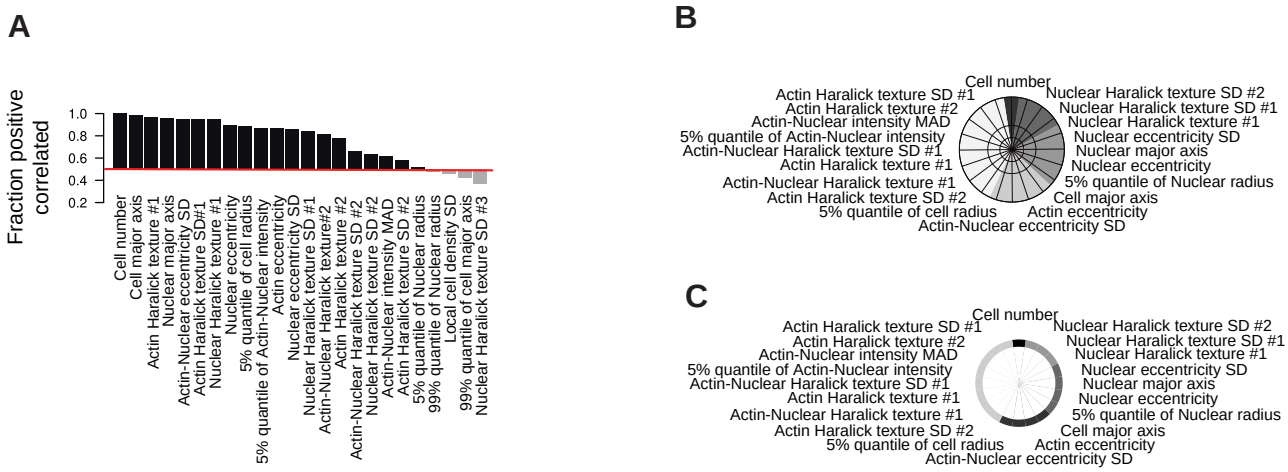

Appendix Figure S2. Phenotypic features.

A Feature names to Figure 1C. Linear decomposition selected a final set of 20 phenotypic features.

B Feature names to Figure 1D. Phenotypic features are grouped in 5 phenotypic categories and span phenoprints.

C Feature names to Figure 2 and 4. Phenotypic interactions for the selected 20 features are grouped in 5 phenotypic categories.

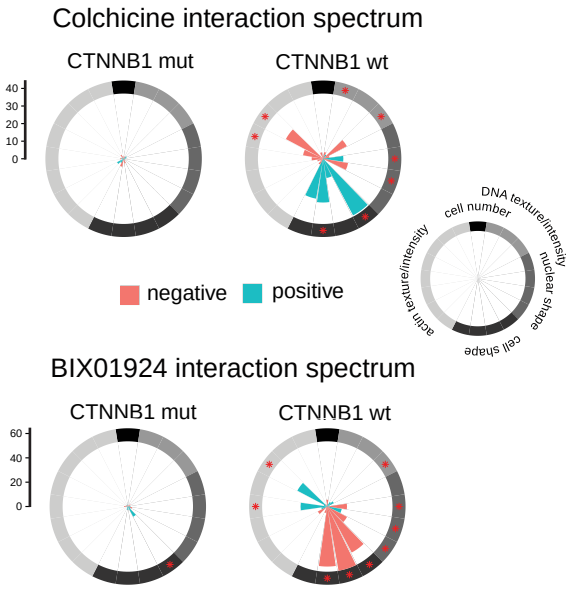

Appendix Figure S3. Quantitative analysis of chemical-genetic interactions across multiple phenotypic features.
Chemical-genetic interactions were calculated for all 20 phenotypic features as described. Colchicine and BIX01294 show multiple interactions in CTNNB1 wt cells. Phenotypic chemo-genomic interactions are shown unscaled. Interactions are further categorized in positive and negative interactions according to the sign of interaction terms (see Material and Methods for details). * adjusted p-value < 0.01.

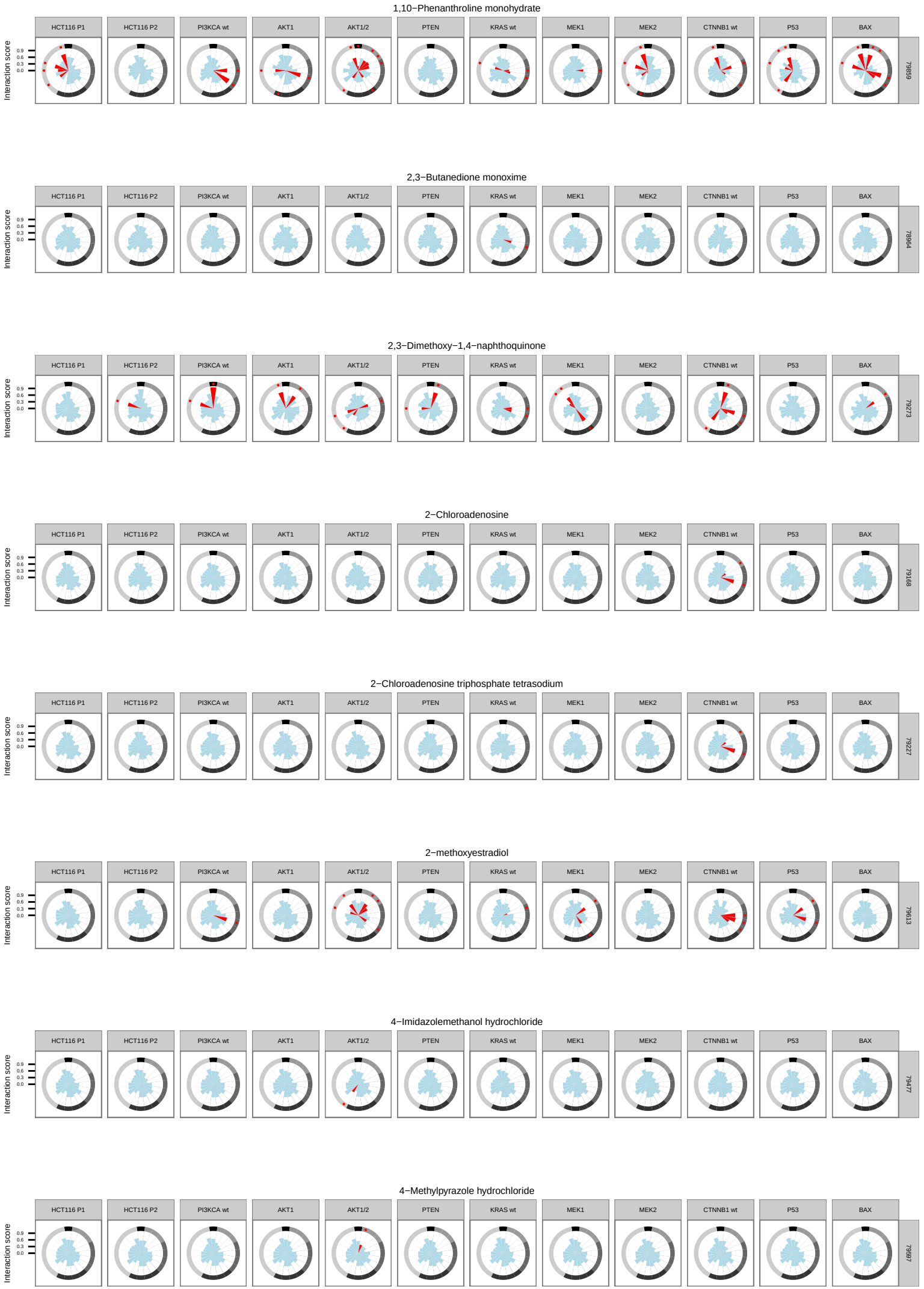
1,10−Phenanthroline monohydrate
2,3−Butanedione monoxime
2,3−Dimethoxy−1,4−naphthoquinone
2−Chloroadenosine
2−Chloroadenosine triphosphate tetrasodium
2−methoxyestradiol
4−Imidazolemethanol hydrochloride
4−Methylpyrazole hydrochloride
HCT116 P1
HCT116 P2
PI3KCA wt
AKT1
AKT1/2
PTEN
KRAS wt
MEK1
MEK2
CTNNB1 wt
P53
BAX
Interaction score
0.9
0.6
0.3
0.0
79859
78964
79273
79168
79227
79613
79477
79987

5−azacytidine

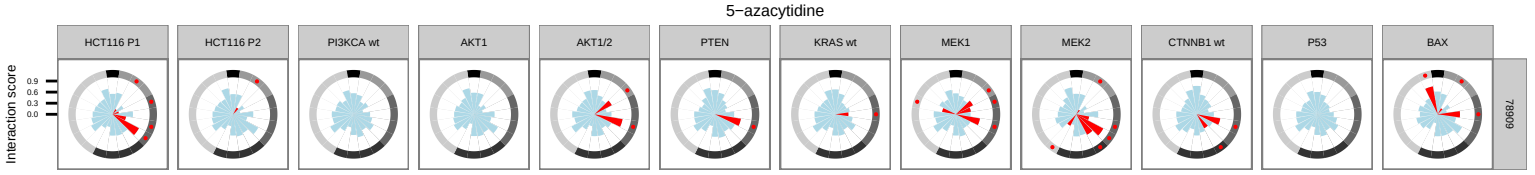

5−Bromo−2'−deoxyuridine

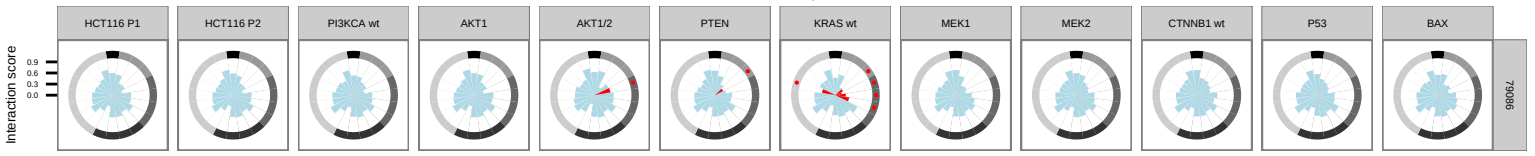

5−fluoro−5'−deoxyuridine

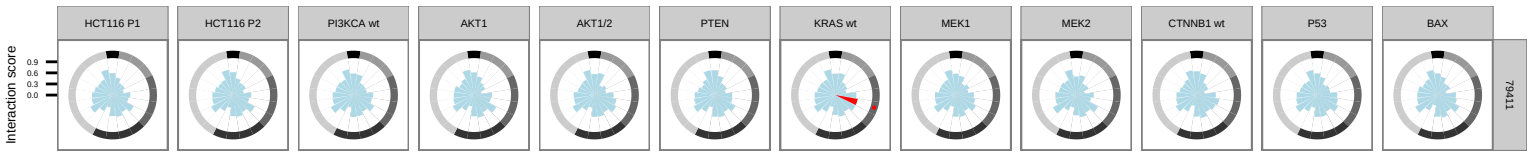

5−Fluorouracil

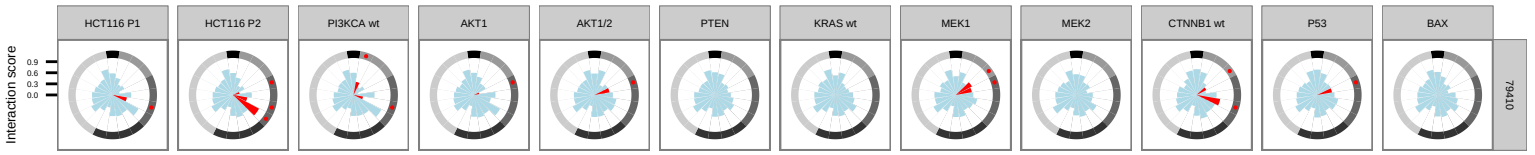

5'−N−Ethylcarboxamidoadenosine

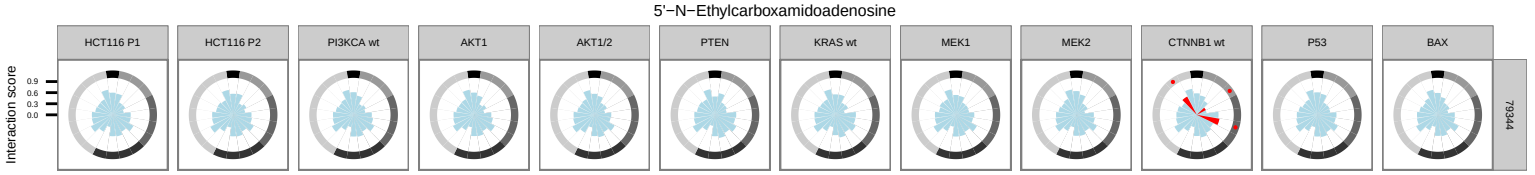

5−(N−Ethyl−N−isopropyl)amiloride

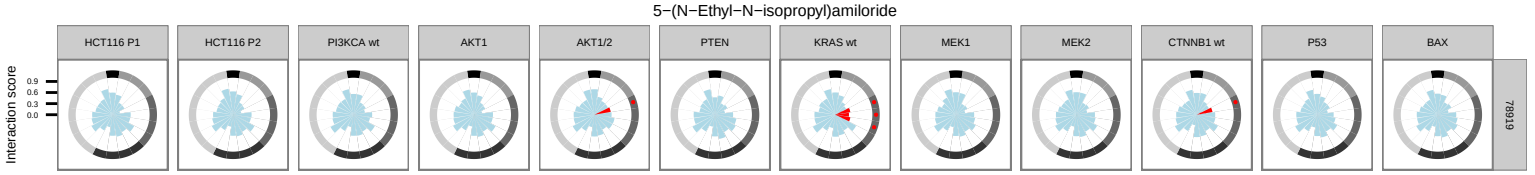

5−(N,N−hexamethylene)amiloride

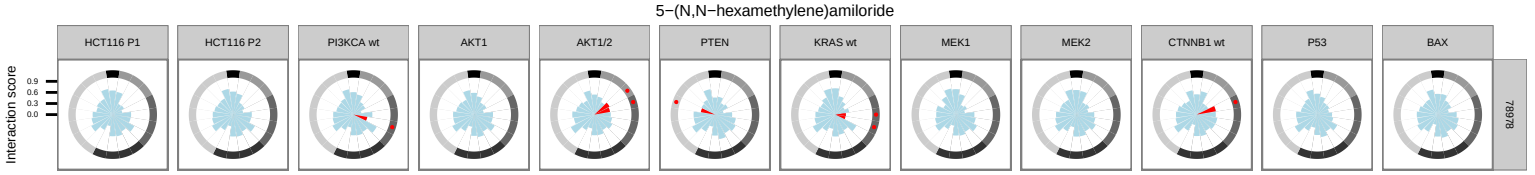

6−Methoxy−1,2,3,4−tetrahydro−9H−pyrido[3,4b] indole

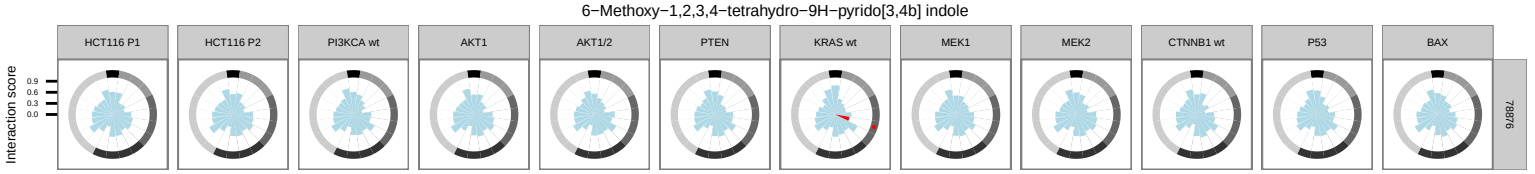

7−Cyclopentyl−5−(4−phenoxy)phenyl−7H−pyrrolo[2,3−d]pyrimidin−4−ylamine

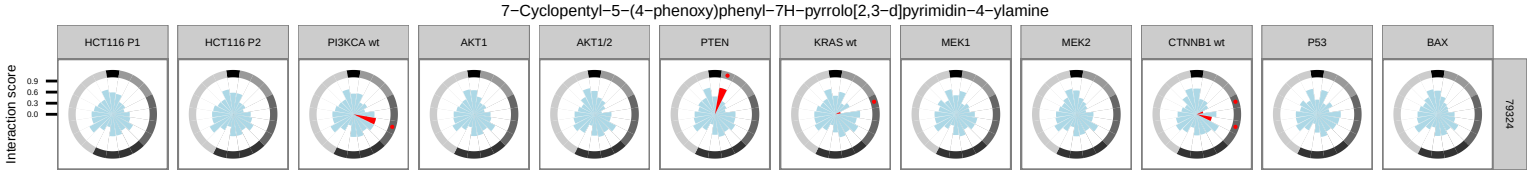

A−134974 dihydrochloride hydrate

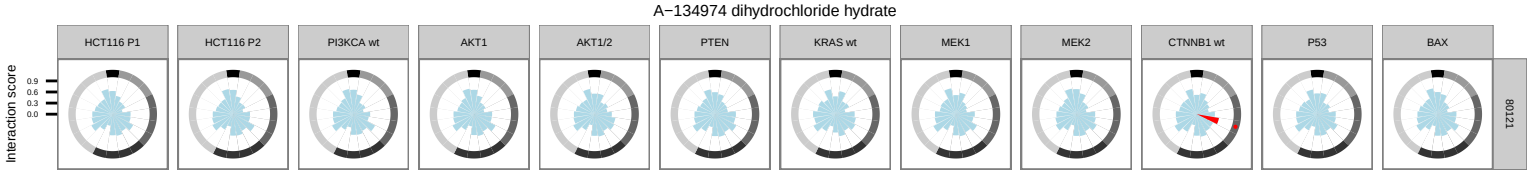

A−77636 hydrochloride

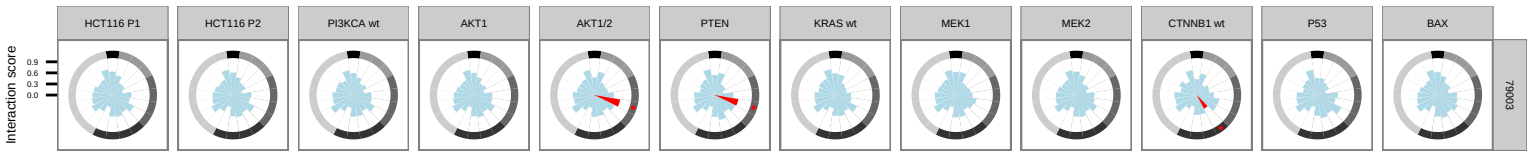

ABT−702 dihydrochloride

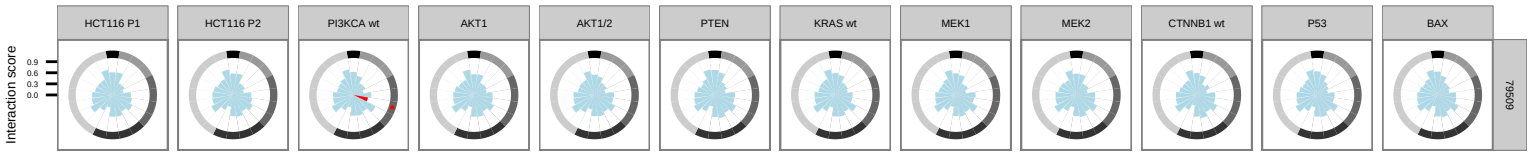

Actinonin

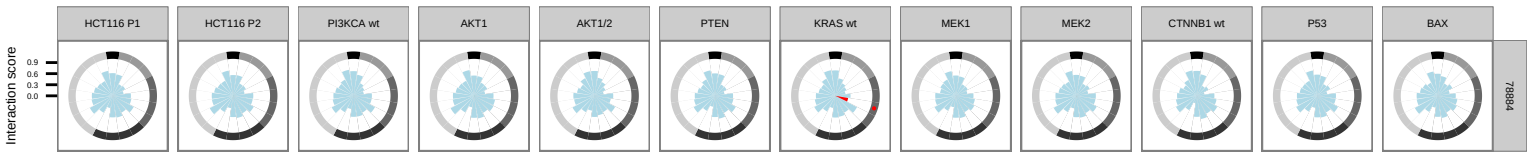

Aminopterin

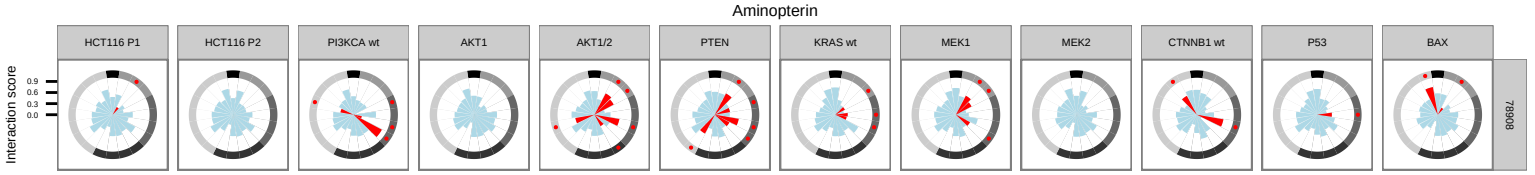

Ammonium pyrrolidinedithiocarbamate

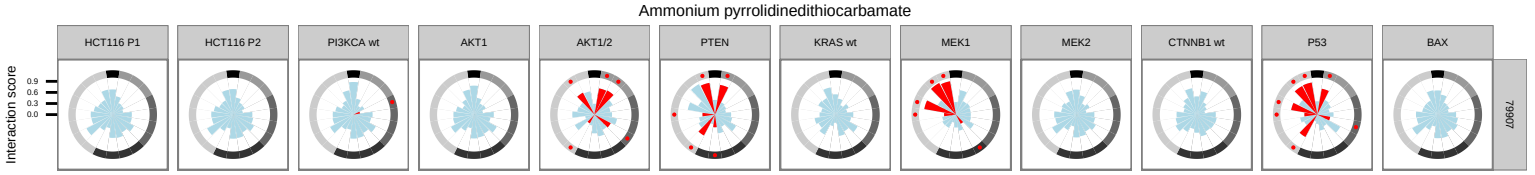

Amoxapine

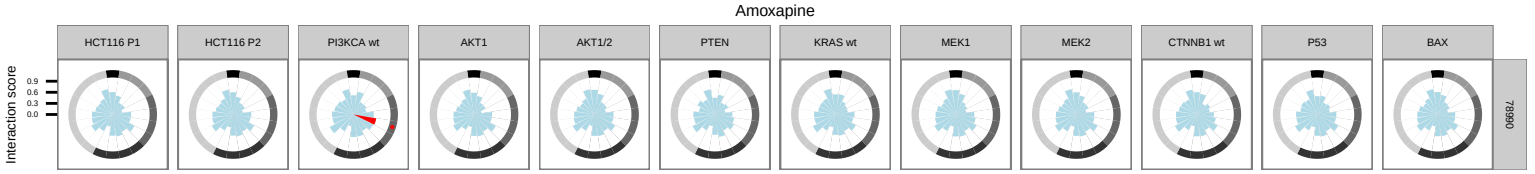

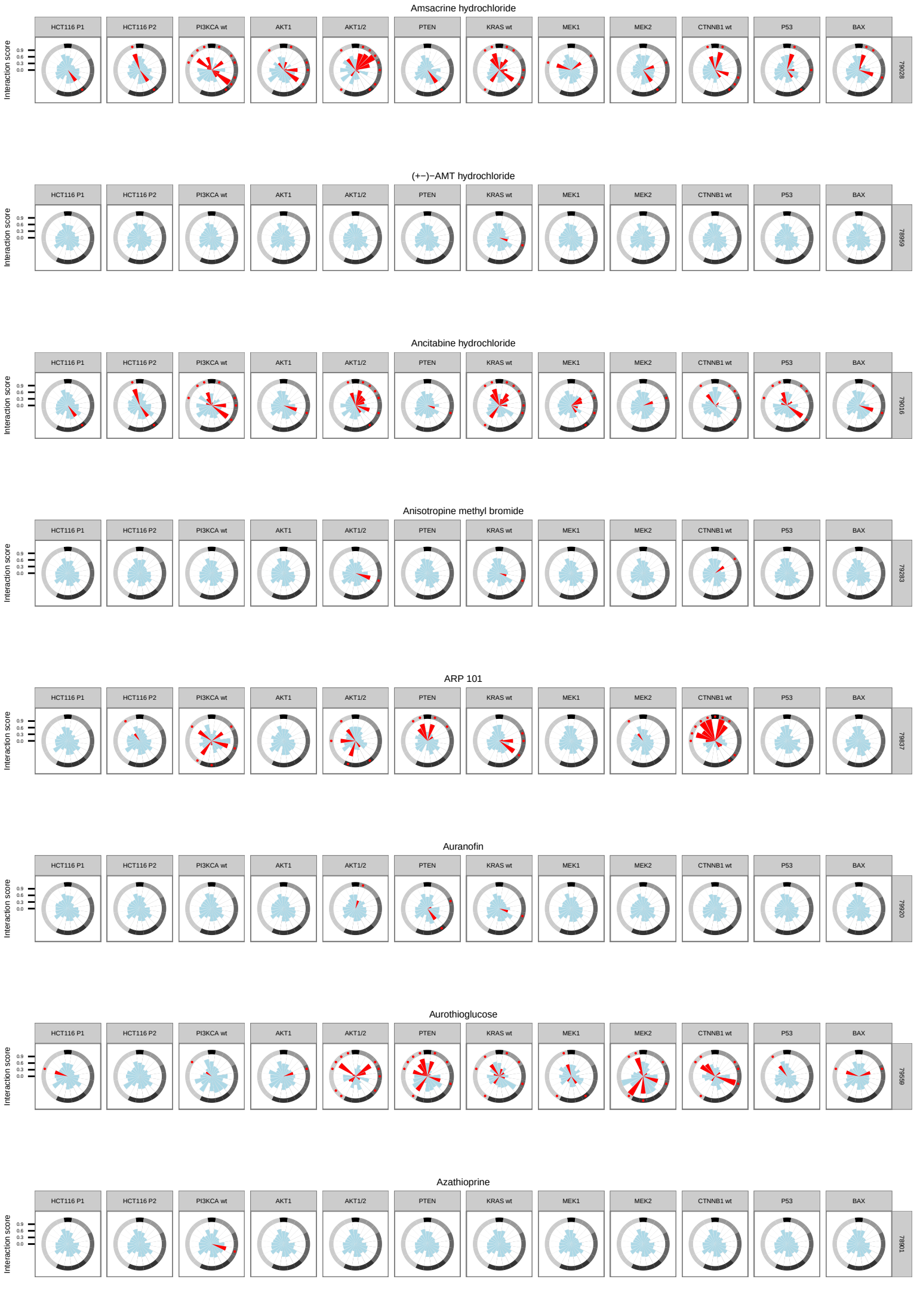
Amsacrine hydrochloride
(+−)−AMT hydrochloride
Ancitabine hydrochloride
Anisotropine methyl bromide
ARP 101
Auranofin
Aurothioglucose
Azathioprine
HCT116 P1
HCT116 P2
PI3KCA wt
AKT1
AKT1/2
PTEN
KRAS wt
MEK1
MEK2
CTNNB1 wt
P53
BAX
Interaction score
0.9
0.6
0.3
0.0
79028
78959
79016
79283
79837
79920
79559
78901

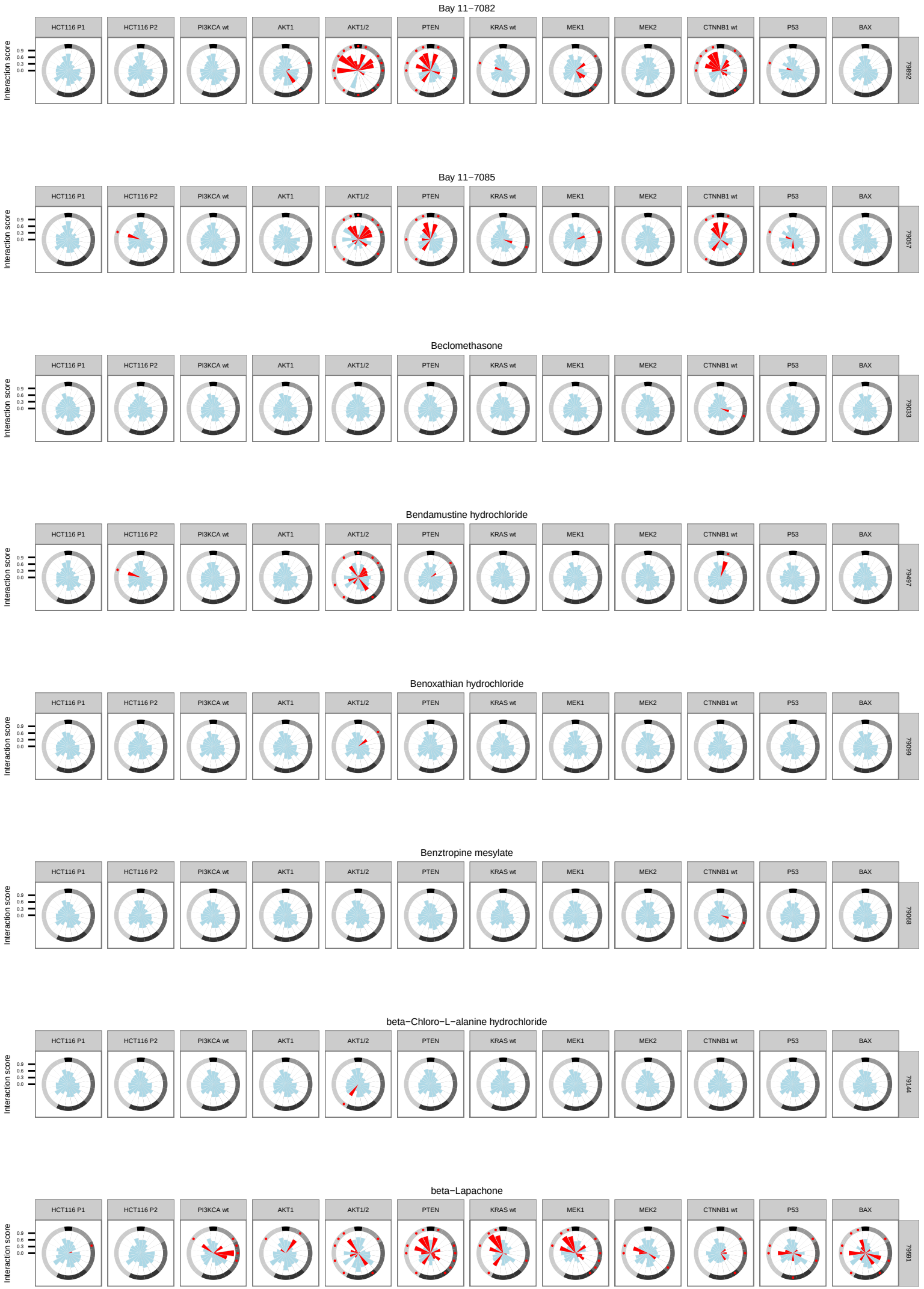
Bay 11−7082
Bay 11−7085
Beclomethasone
Bendamustine hydrochloride
Benoxathian hydrochloride
Benztropine mesylate
beta−Chloro−L−alanine hydrochloride
beta−Lapachone
HCT116 P1
HCT116 P2
PI3KCA wt
AKT1
AKT1/2
PTEN
KRAS wt
MEK1
MEK2
CTNNB1 wt
P53
BAX
Interaction score
0.0
0.3
0.6
0.9
79892
79057
79033
79497
79099
79068
79144
79991

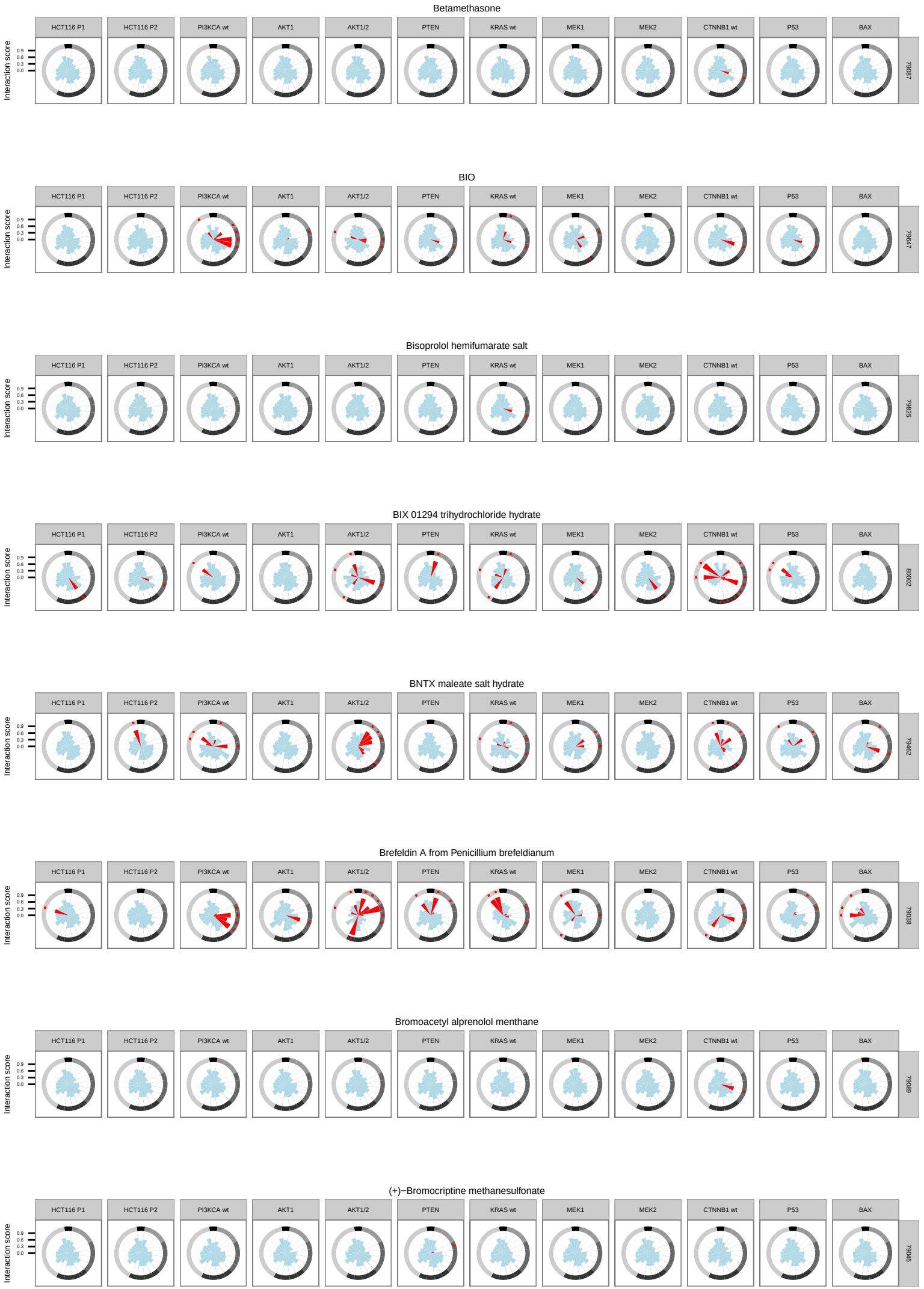
Betamethasone
BIO
Bisoprolol hemifumarate salt
BIX 01294 trihydrochloride hydrate
BNTX maleate salt hydrate
Brefeldin A from Penicillium brefeldianum
Bromoacetyl alprenolol menthane
(+)−Bromocriptine methanesulfonate
HCT116 P1
HCT116 P2
PI3KCA wt
AKT1
AKT1/2
PTEN
KRAS wt
MEK1
MEK2
CTNNB1 wt
P53
BAX
Interaction score
0.9
0.6
0.3
0.0
79087
79647
79825
80002
79462
79038
79089
79045

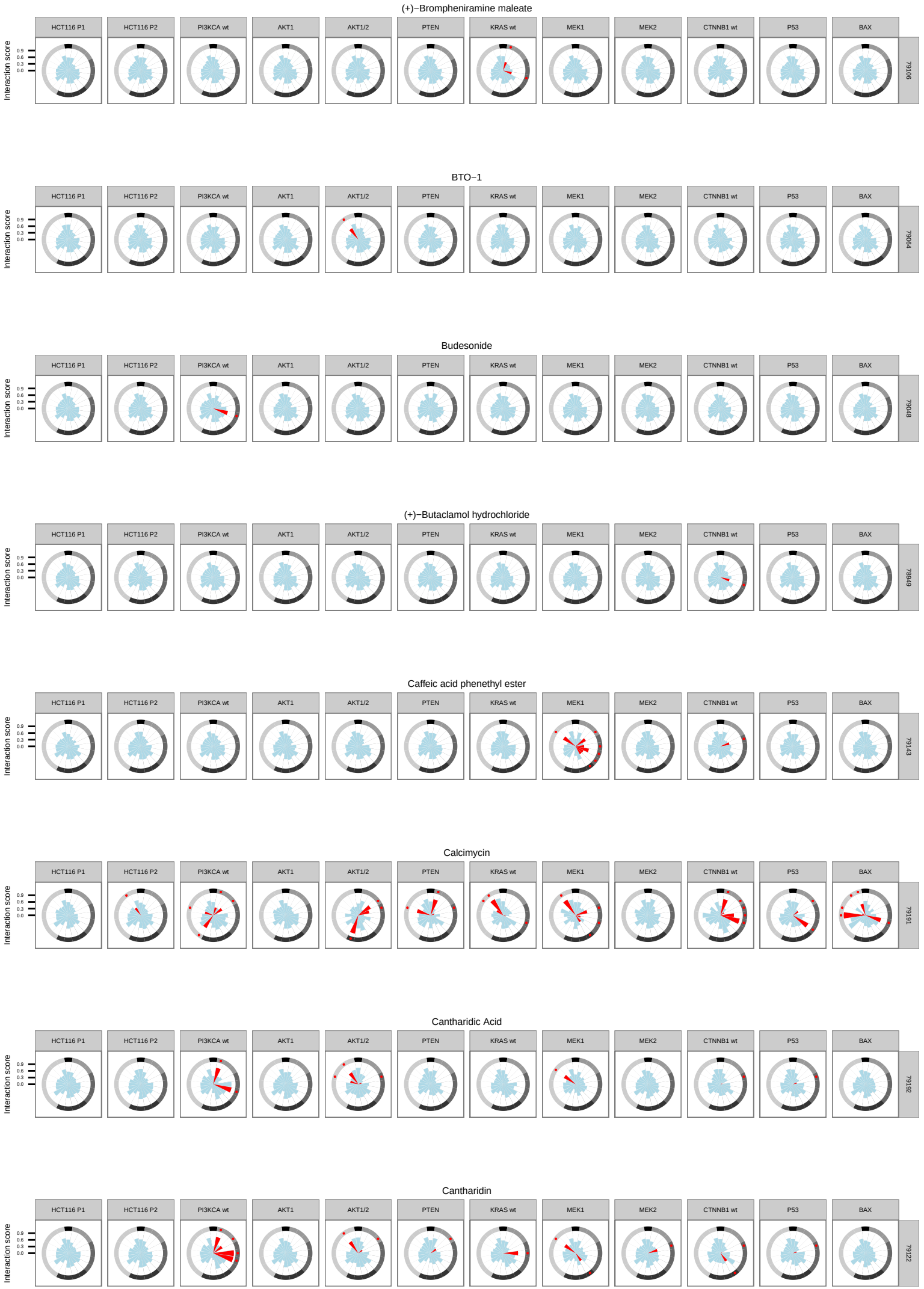
(+)−Brompheniramine maleate
BTO−1
Budesonide
(+)−Butaclamol hydrochloride
Caffeic acid phenethyl ester
Calcimycin
Cantharidic Acid
Cantharidin
HCT116 P1
HCT116 P2
PI3KCA wt
AKT1
AKT1/2
PTEN
KRAS wt
MEK1
MEK2
CTNNB1 wt
P53
BAX
Interaction score
0.9
0.6
0.3
0.0
79106
79064
79048
79049
79143
79191
79192
79122

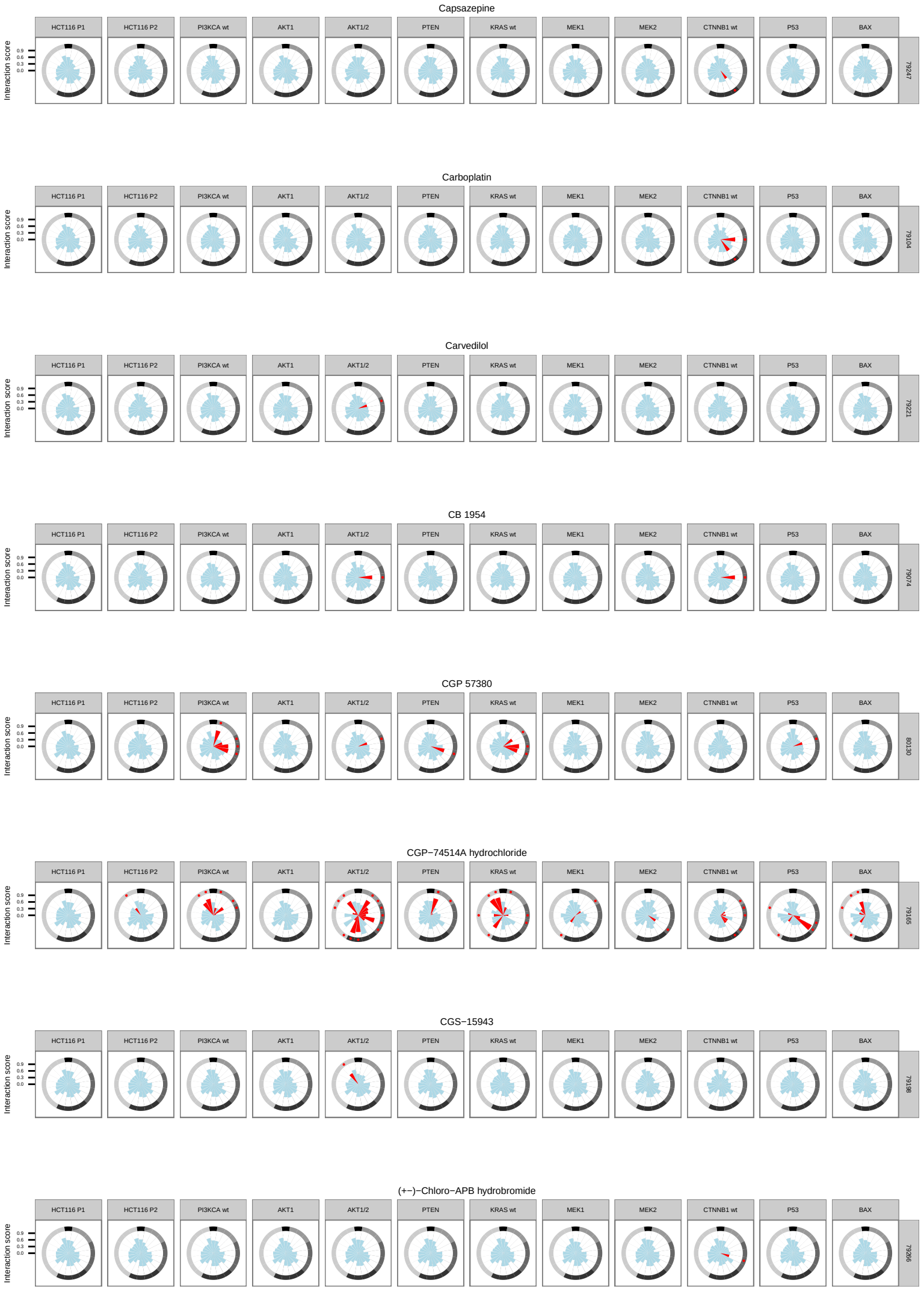
Capsazepine
Carboplatin
Carvedilol
CB 1954
CGP 57380
CGP−74514A hydrochloride
CGS−15943
(+−)−Chloro−APB hydrobromide
HCT116 P1
HCT116 P2
PI3KCA wt
AKT1
AKT1/2
PTEN
KRAS wt
MEK1
MEK2
CTNNB1 wt
P53
BAX
Interaction score
0.9
0.6
0.3
0.0
79247
79104
79221
79074
80130
79165
79198
79266

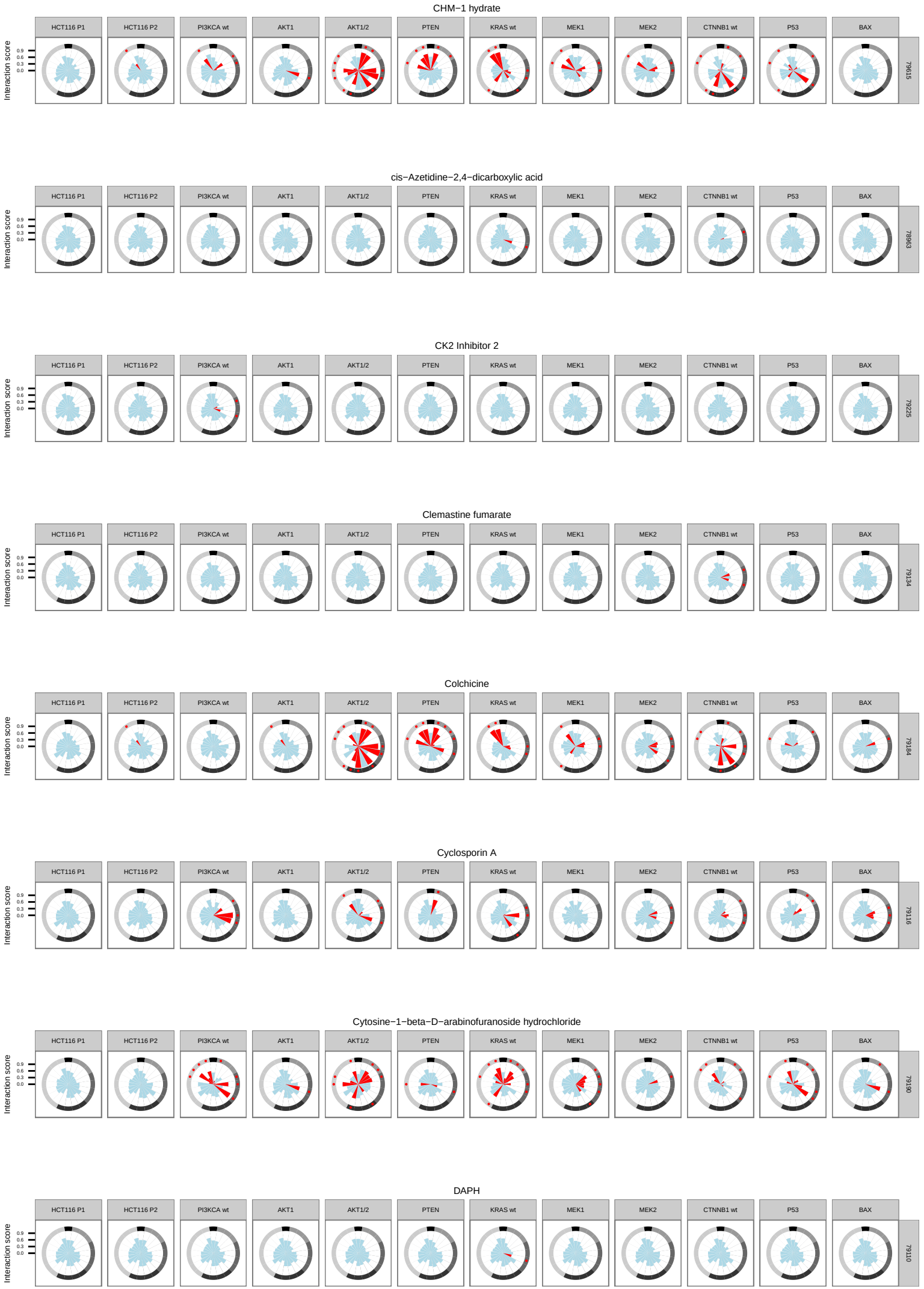
CHM−1 hydrate
cis−Azetidine−2,4−dicarboxylic acid
CK2 Inhibitor 2
Clemastine fumarate
Colchicine
Cyclosporin A
Cytosine−1−beta−D−arabinofuranoside hydrochloride
DAPH
HCT116 P1
HCT116 P2
PI3KCA wt
AKT1
AKT1/2
PTEN
KRAS wt
MEK1
MEK2
CTNNB1 wt
P53
BAX
Interaction score
0.9
0.6
0.3
0.0
79615
78963
79225
79134
79184
79116
79190
79110

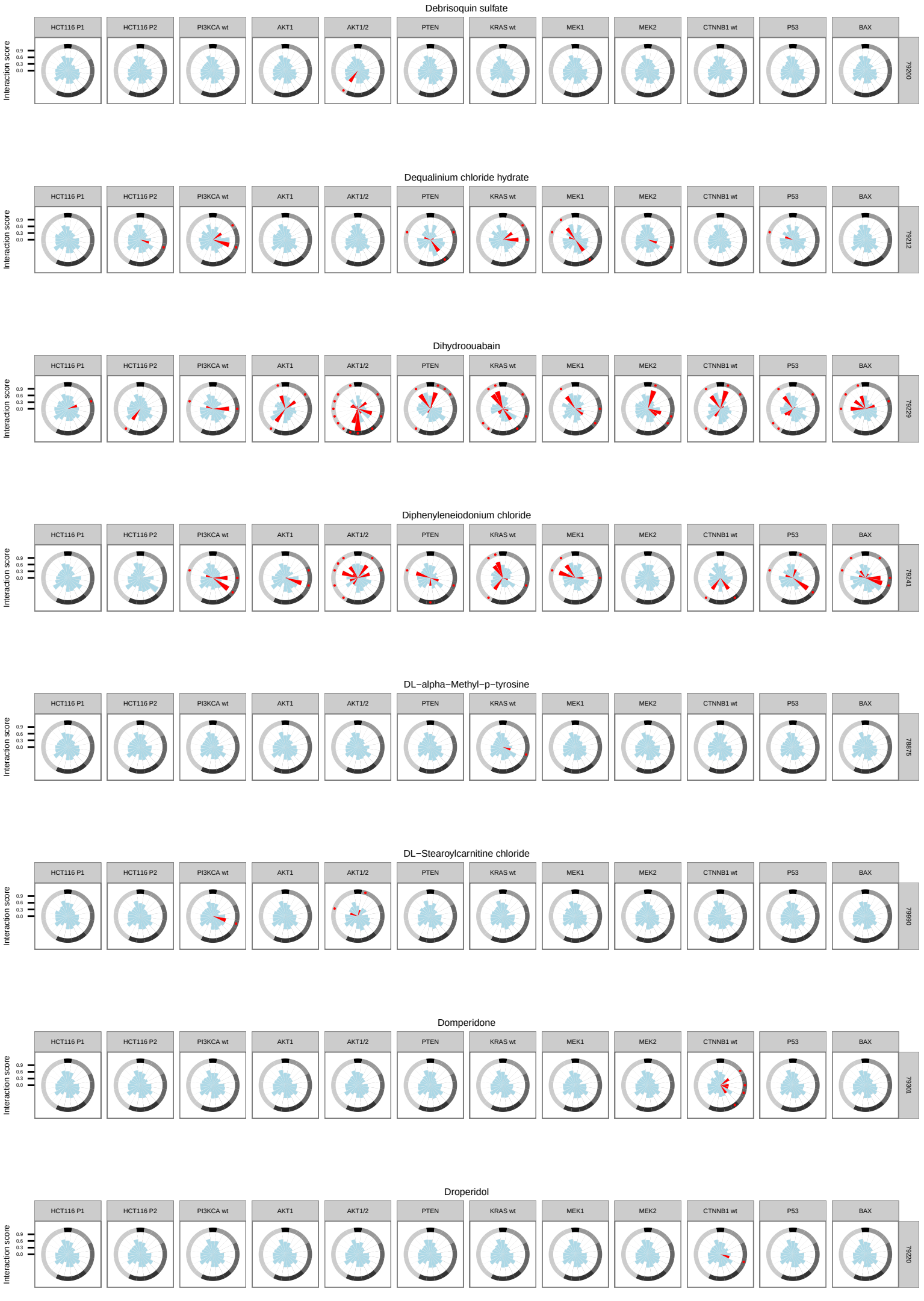
Debrisoquin sulfate
Dequalinium chloride hydrate
Dihydroouabain
Diphenyleneiodonium chloride
DL−alpha−Methyl−p−tyrosine
DL−Stearoylcarnitine chloride
Domperidone
Droperidol
HCT116 P1
HCT116 P2
PI3KCA wt
AKT1
AKT1/2
PTEN
KRAS wt
MEK1
MEK2
CTNNB1 wt
P53
BAX
Interaction score
0.9
0.6
0.3
0.0
79200
79212
79229
79241
78875
79990
79301
79220

(E)−5−(2−Bromovinyl)−2'−deoxyuridine

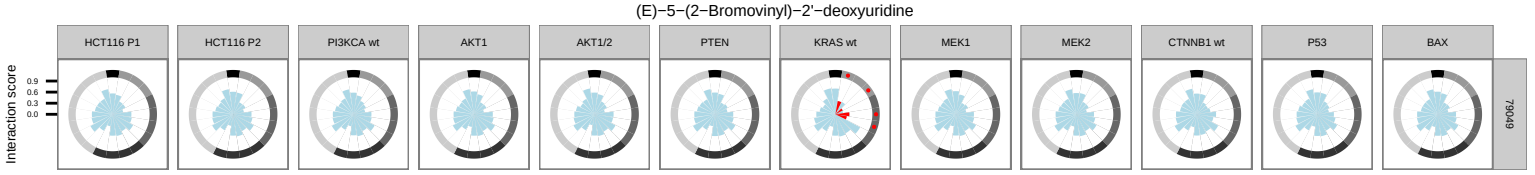

EGTA

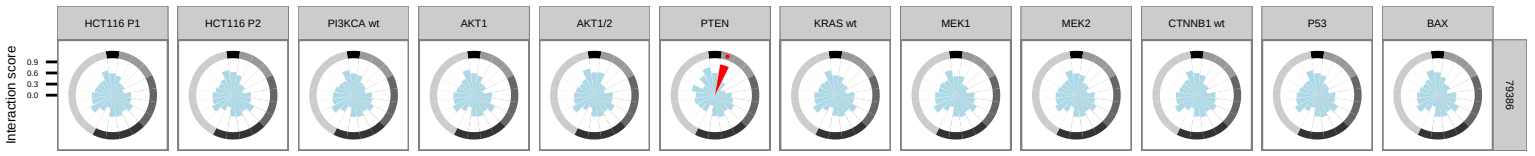

Ellipticine

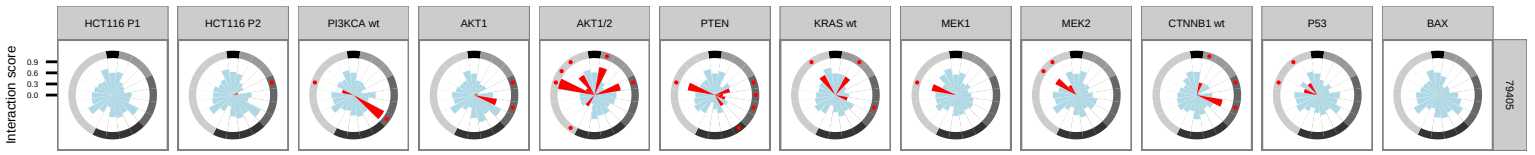

Emetine dihydrochloride hydrate

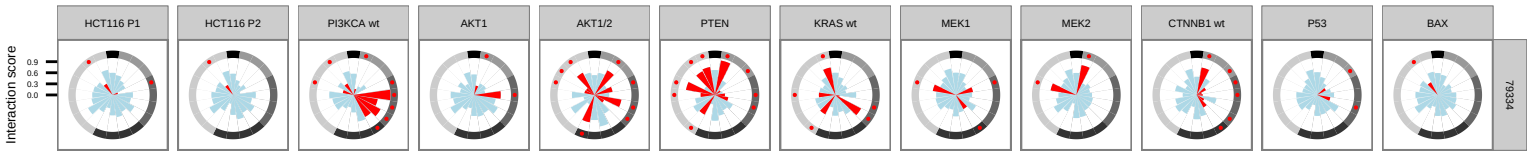

Enalaprilat dihydrate

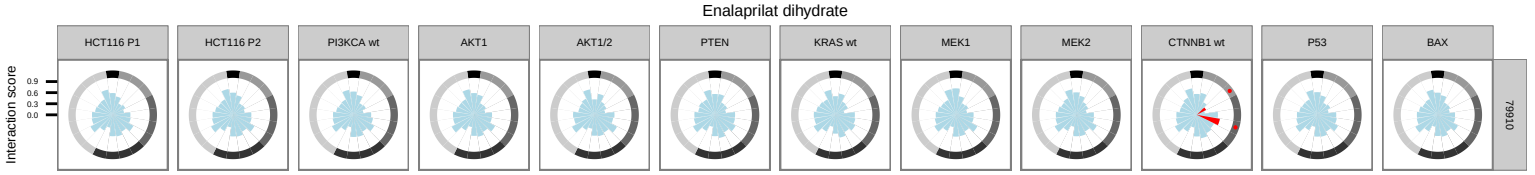

ET−18−OCH3

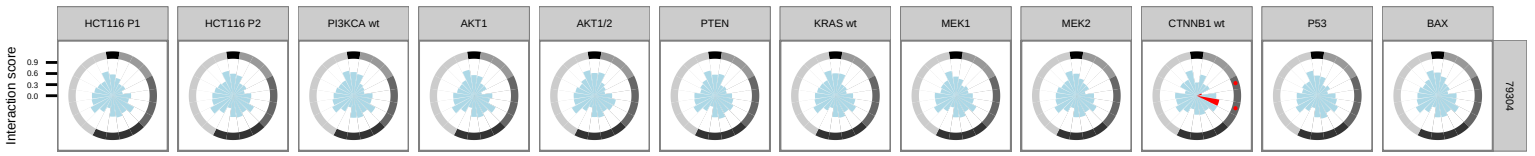

Ethopropazine hydrochloride

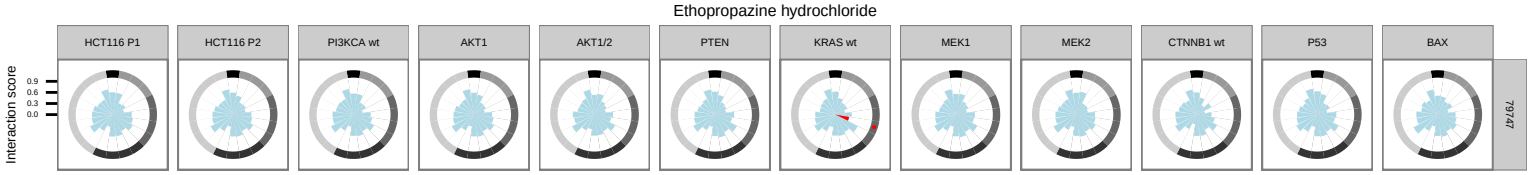

Etoposide

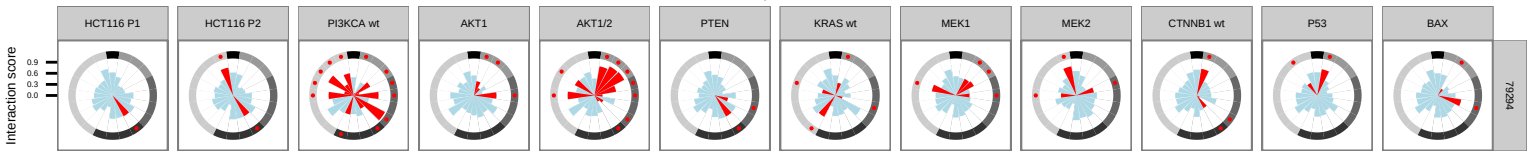

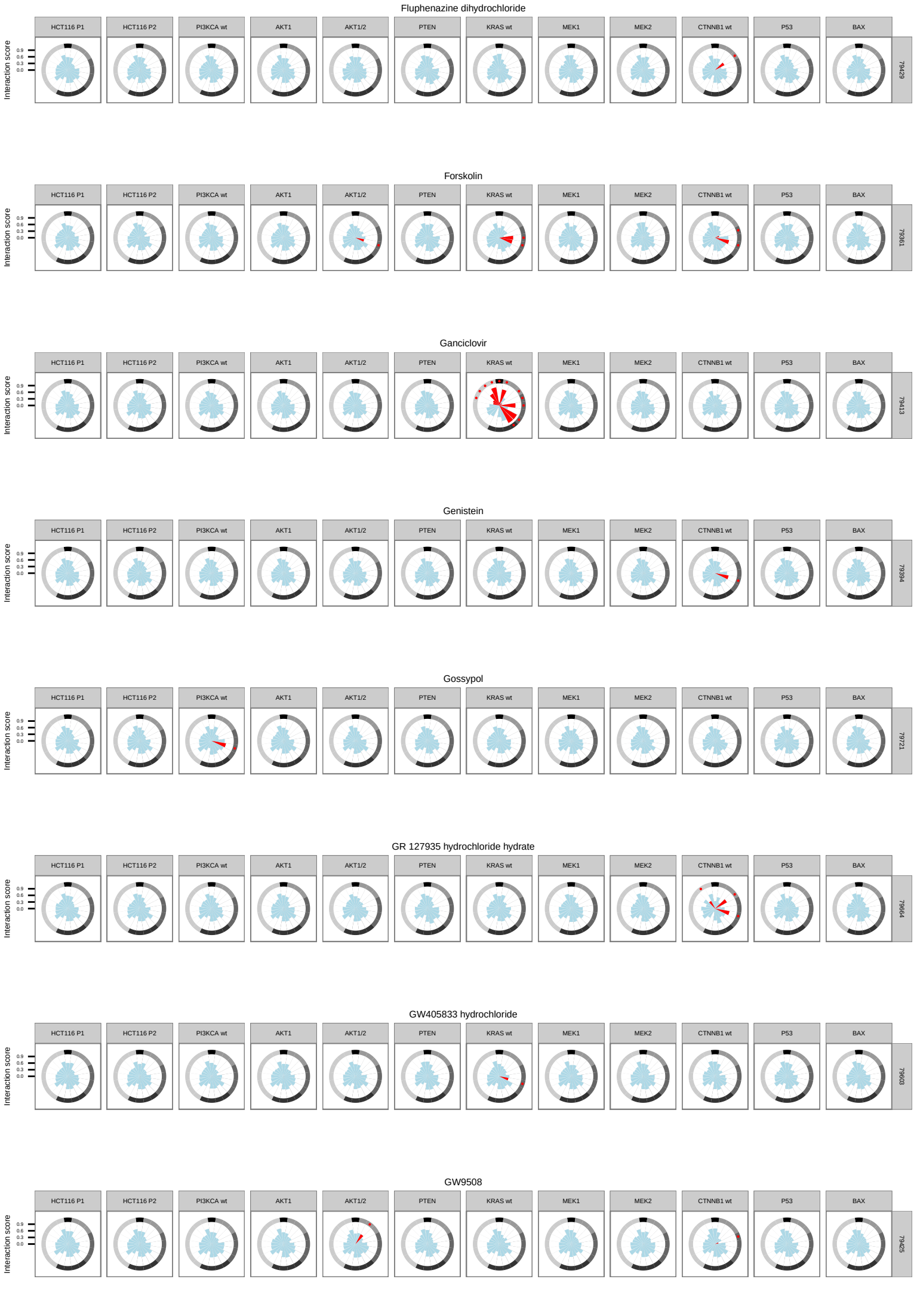
Fluphenazine dihydrochloride
Forskolin
Ganciclovir
Genistein
Gossypol
GR 127935 hydrochloride hydrate
GW405833 hydrochloride
GW9508
HCT116 P1
HCT116 P2
PI3KCA wt
AKT1
AKT1/2
PTEN
KRAS wt
MEK1
MEK2
CTNNB1 wt
P53
BAX
Interaction score
0.9
0.6
0.3
0.0
79429
79361
79413
79394
79721
79664
79603
79425

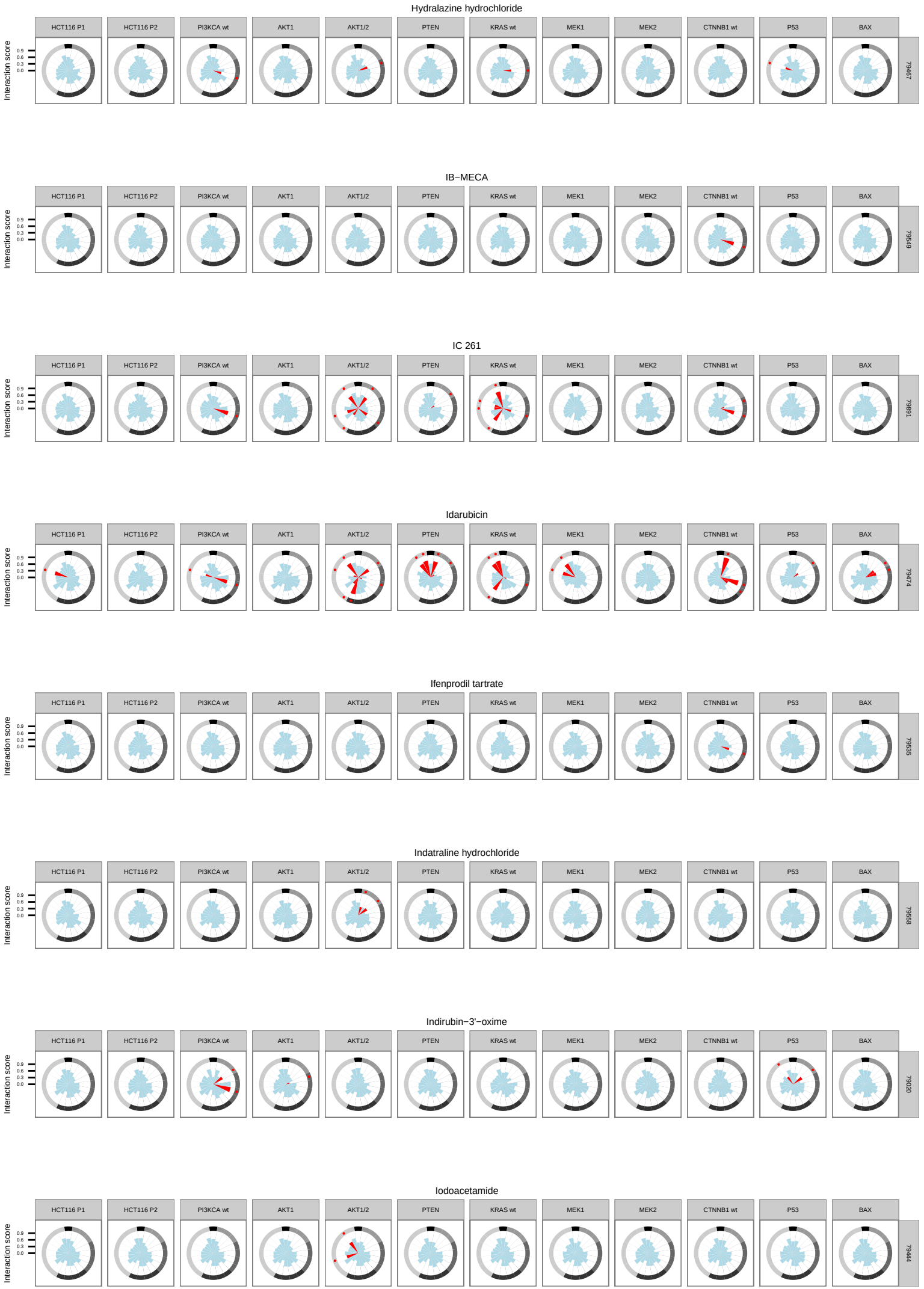
Hydralazine hydrochloride
IB−MECA
IC 261
Idarubicin
Ifenprodil tartrate
Indatraline hydrochloride
Indirubin−3'−oxime
Iodoacetamide
HCT116 P1
HCT116 P2
PI3KCA wt
AKT1
AKT1/2
PTEN
KRAS wt
MEK1
MEK2
CTNNB1 wt
P53
BAX
Interaction score
0.9
0.6
0.3
0.0
79467
79549
79891
79474
79535
79558
79020
79444

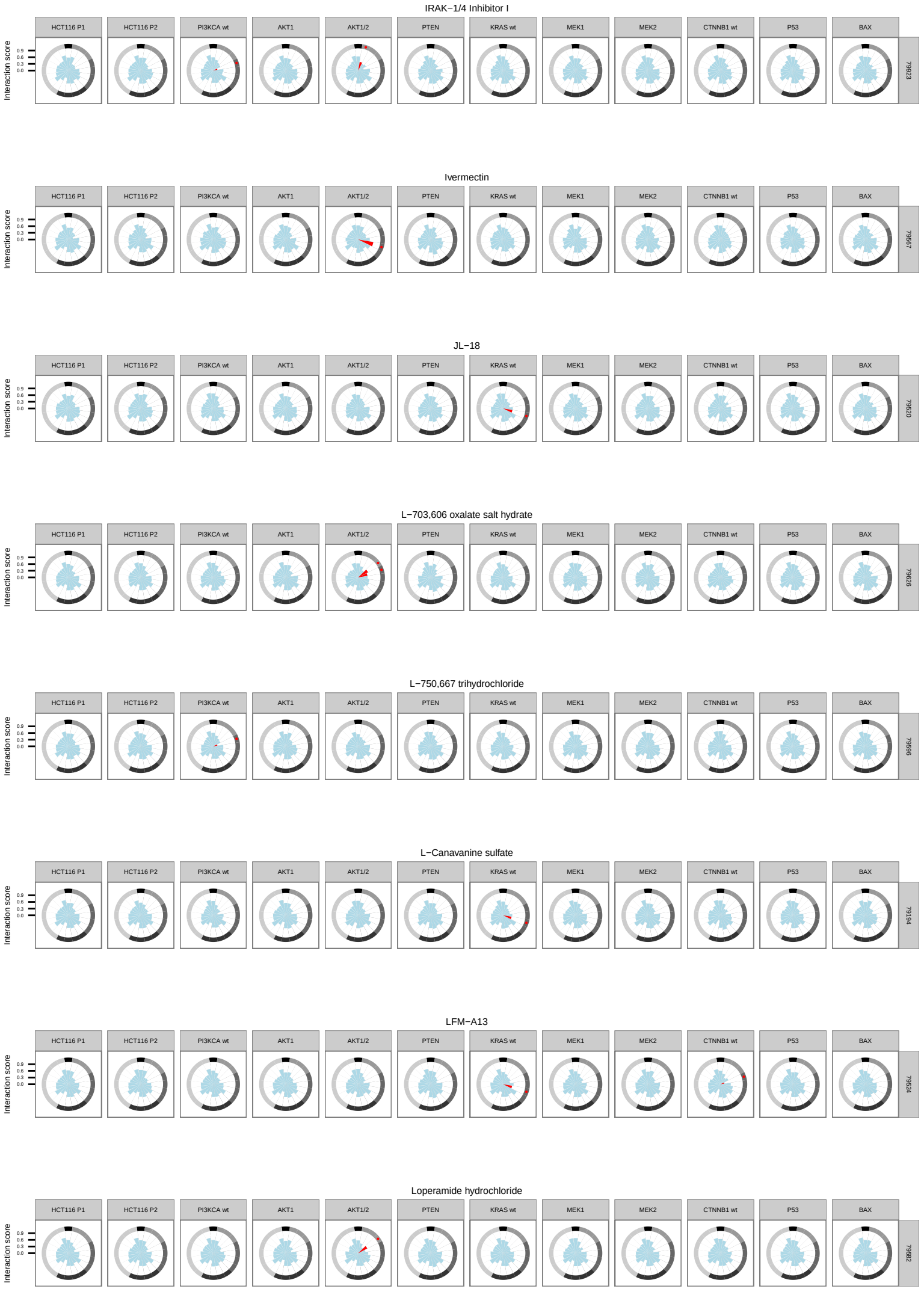
IRAK−1/4 Inhibitor I
Ivermectin
JL−18
L−703,606 oxalate salt hydrate
L−750,667 trihydrochloride
L−Canavanine sulfate
LFM−A13
Loperamide hydrochloride
HCT116 P1
HCT116 P2
PI3KCA wt
AKT1
AKT1/2
PTEN
KRAS wt
MEK1
MEK2
CTNNB1 wt
P53
BAX
Interaction score
0.9
0.6
0.3
0.0
79923
79567
79520
79626
79596
79194
79524
79582

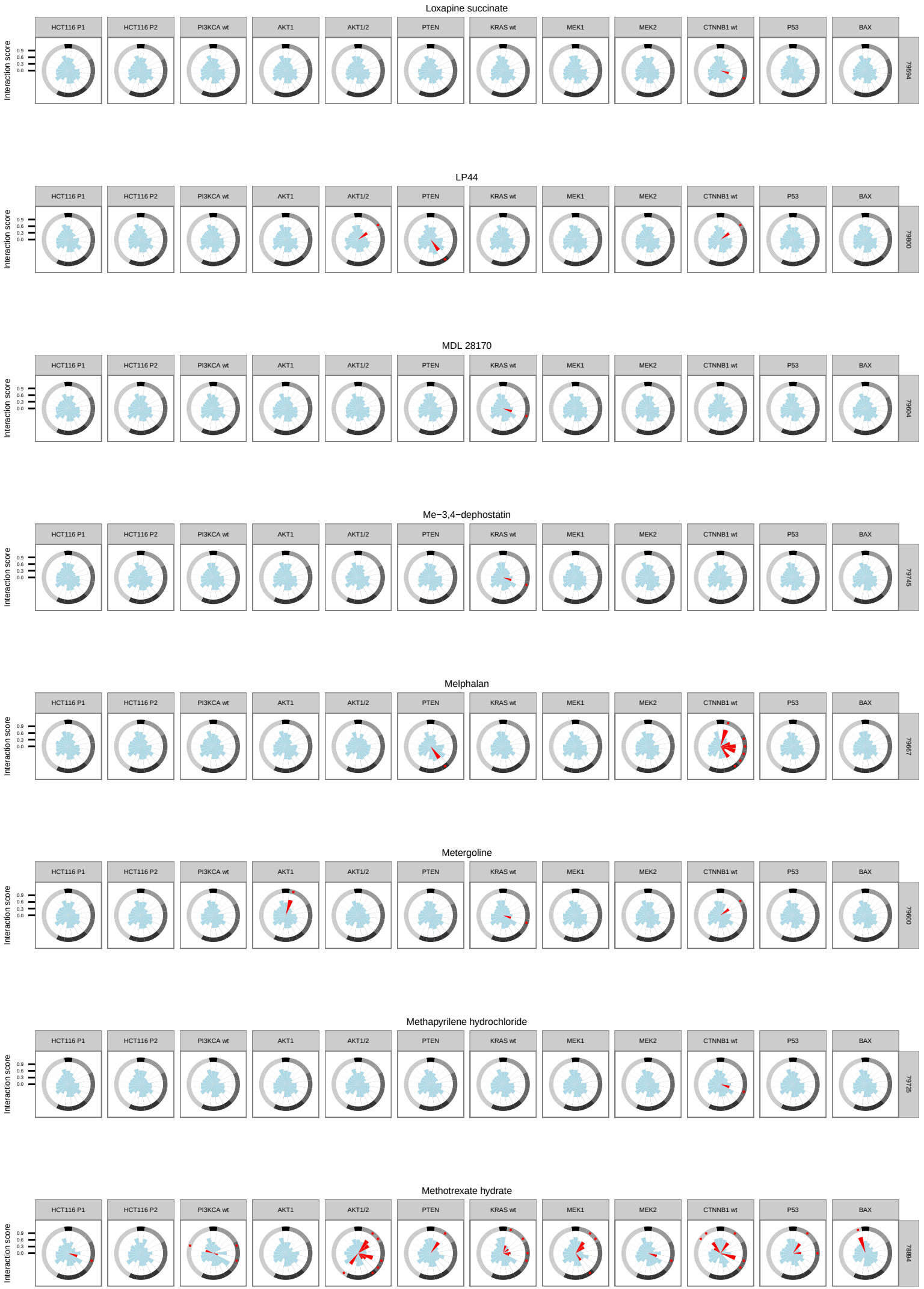
Loxapine succinate
LP44
MDL 28170
Me−3,4−dephostatin
Melphalan
Metergoline
Methapyrilene hydrochloride
Methotrexate hydrate
HCT116 P1
HCT116 P2
PI3KCA wt
AKT1
AKT1/2
PTEN
KRAS wt
MEK1
MEK2
CTNNB1 wt
P53
BAX
Interaction score
0.9
0.6
0.3
0.0
79594
79800
79604
79745
79667
79600
79725
78884

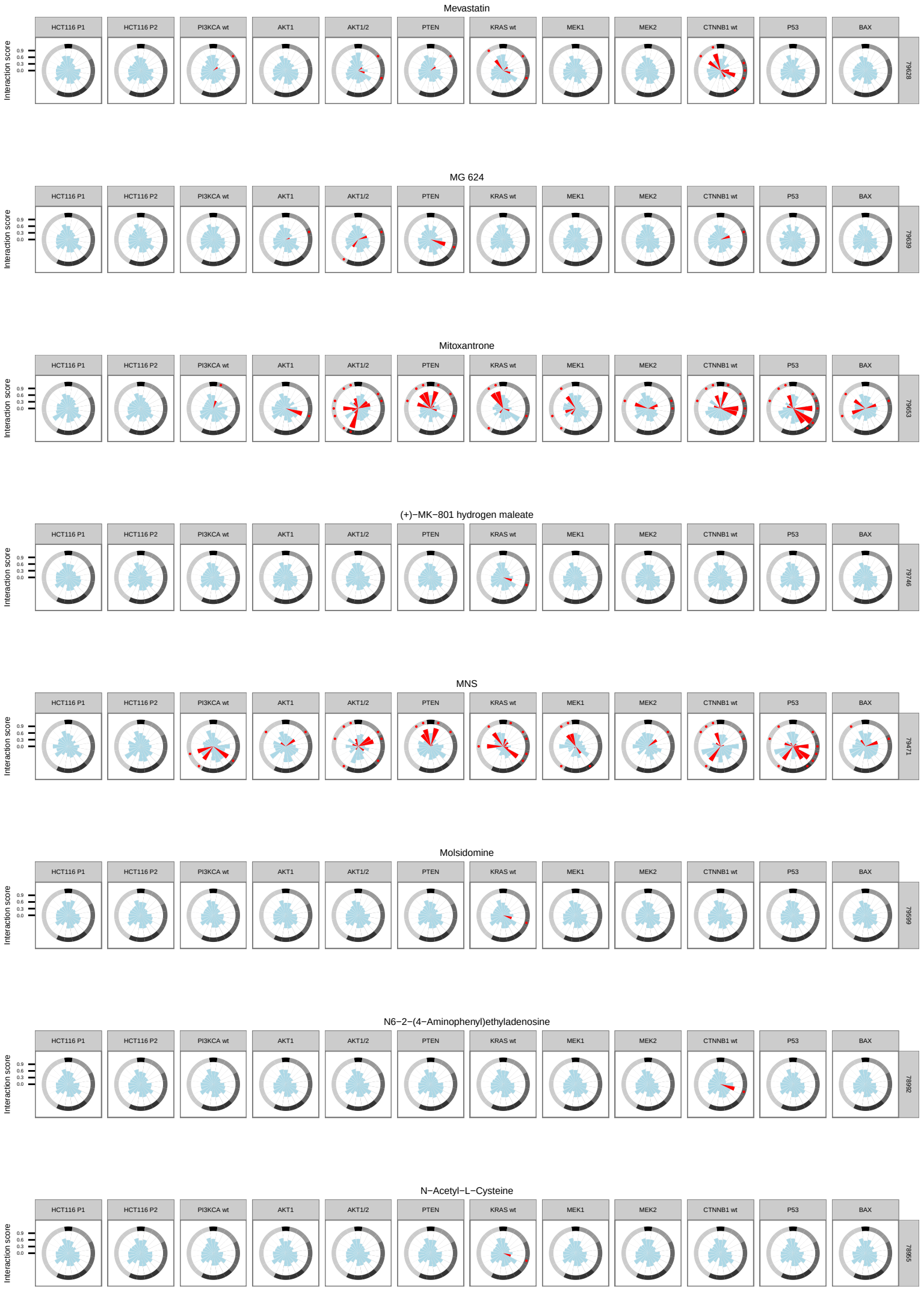
Mevastatin
MG 624
Mitoxantrone
(+)−MK−801 hydrogen maleate
MNS
Molsidomine
N6−2−(4−Aminophenyl)ethyladenosine
N−Acetyl−L−Cysteine
HCT116 P1
HCT116 P2
PI3KCA wt
AKT1
AKT1/2
PTEN
KRAS wt
MEK1
MEK2
CTNNB1 wt
P53
BAX
Interaction score
0.9
0.6
0.3
0.0
79628
79639
79653
79746
79471
79599
78992
78955

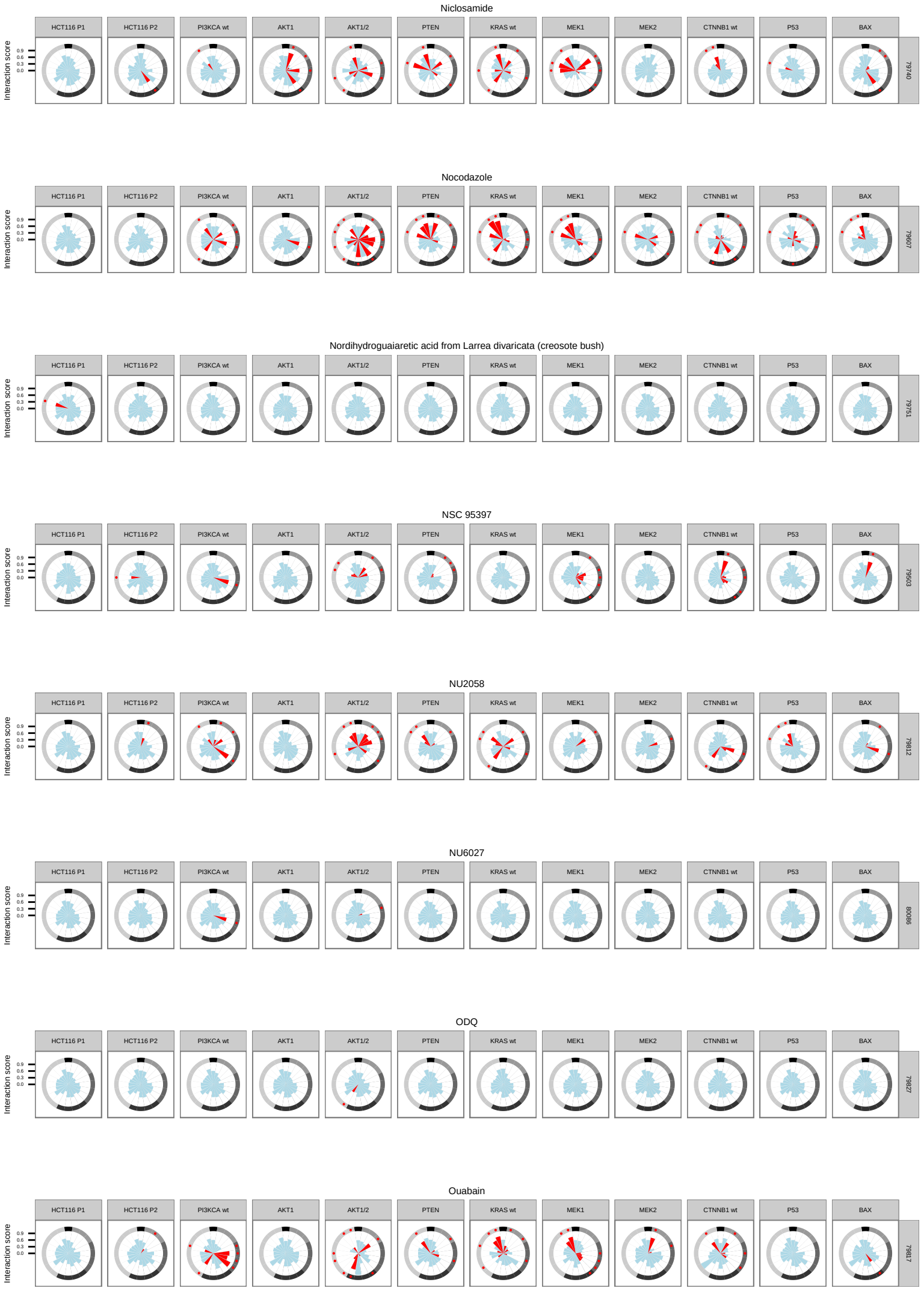
Niclosamide
Nocodazole
Nordihydroguaiaretic acid from Larrea divaricata (creosote bush)
NSC 95397
NU2058
NU6027
ODQ
Ouabain
HCT116 P1
HCT116 P2
PI3KCA wt
AKT1
AKT1/2
PTEN
KRAS wt
MEK1
MEK2
CTNNB1 wt
P53
BAX
Interaction score
0.9
0.6
0.3
0.0
79740
79607
79751
79503
79812
80086
79827
79817

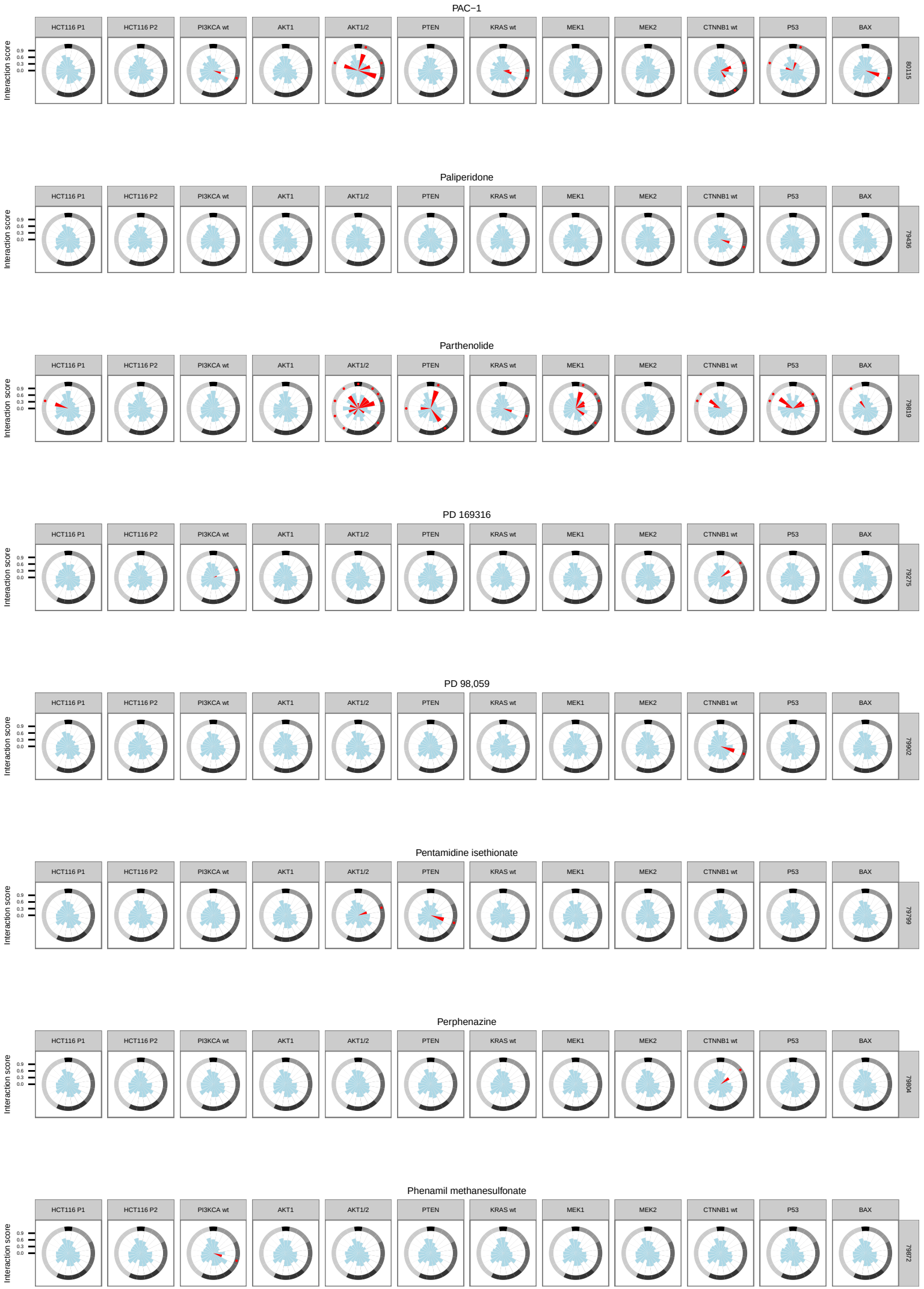
PAC−1
Paliperidone
Parthenolide
PD 169316
PD 98,059
Pentamidine isethionate
Perphenazine
Phenamil methanesulfonate
HCT116 P1
HCT116 P2
PI3KCA wt
AKT1
AKT1/2
PTEN
KRAS wt
MEK1
MEK2
CTNNB1 wt
P53
BAX
Interaction score
0.9
0.6
0.3
0.0
80115
79436
79819
79275
79902
79799
79804
79872

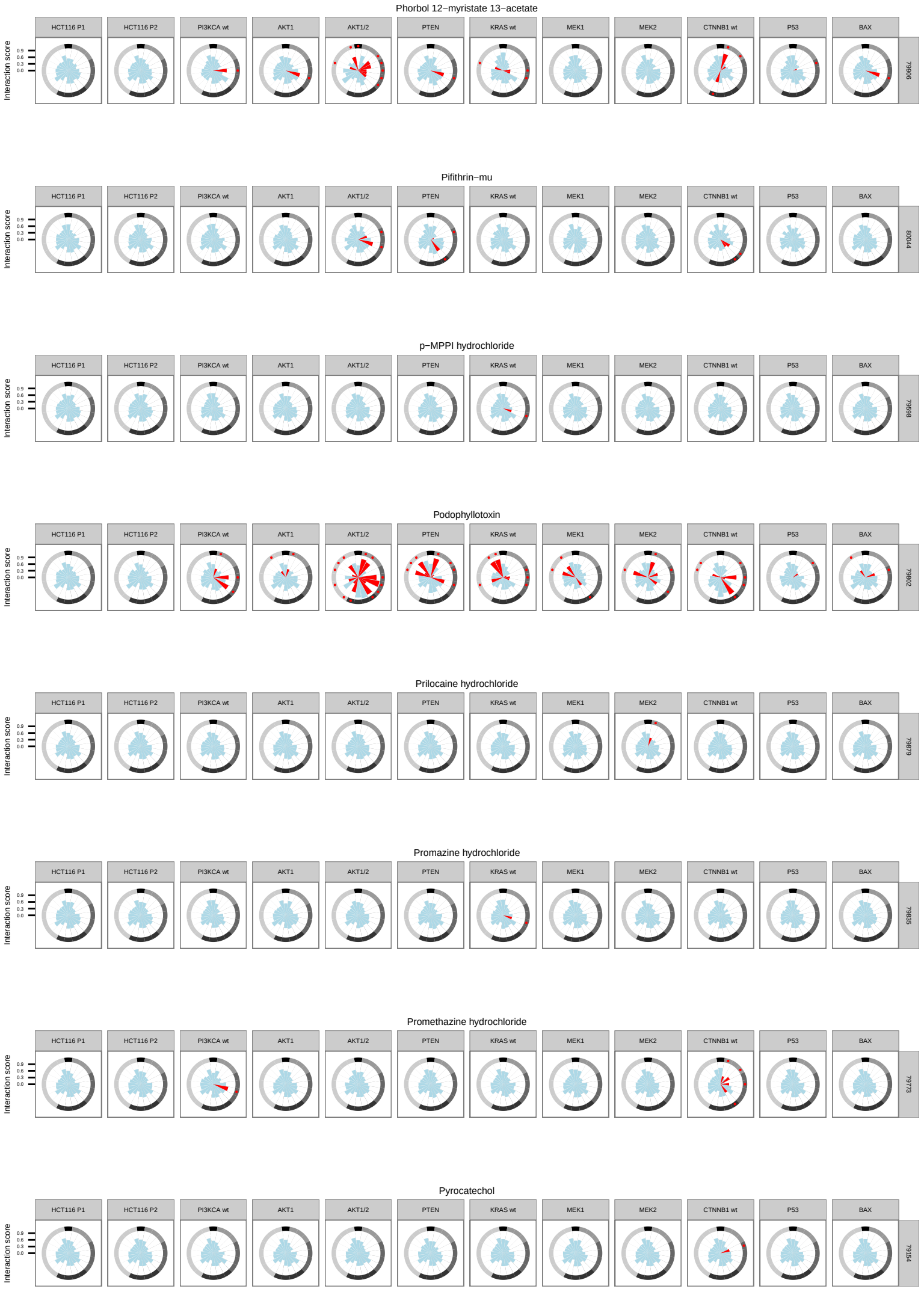
Phorbol 12−myristate 13−acetate
Pifithrin−mu
p−MPPI hydrochloride
Podophyllotoxin
Prilocaine hydrochloride
Promazine hydrochloride
Promethazine hydrochloride
Pyrocatechol
HCT116 P1
HCT116 P2
PI3KCA wt
AKT1
AKT1/2
PTEN
KRAS wt
MEK1
MEK2
CTNNB1 wt
P53
BAX
Interaction score
0.9
0.6
0.3
0.0
79906
80044
79598
79802
79879
79835
79773
79154

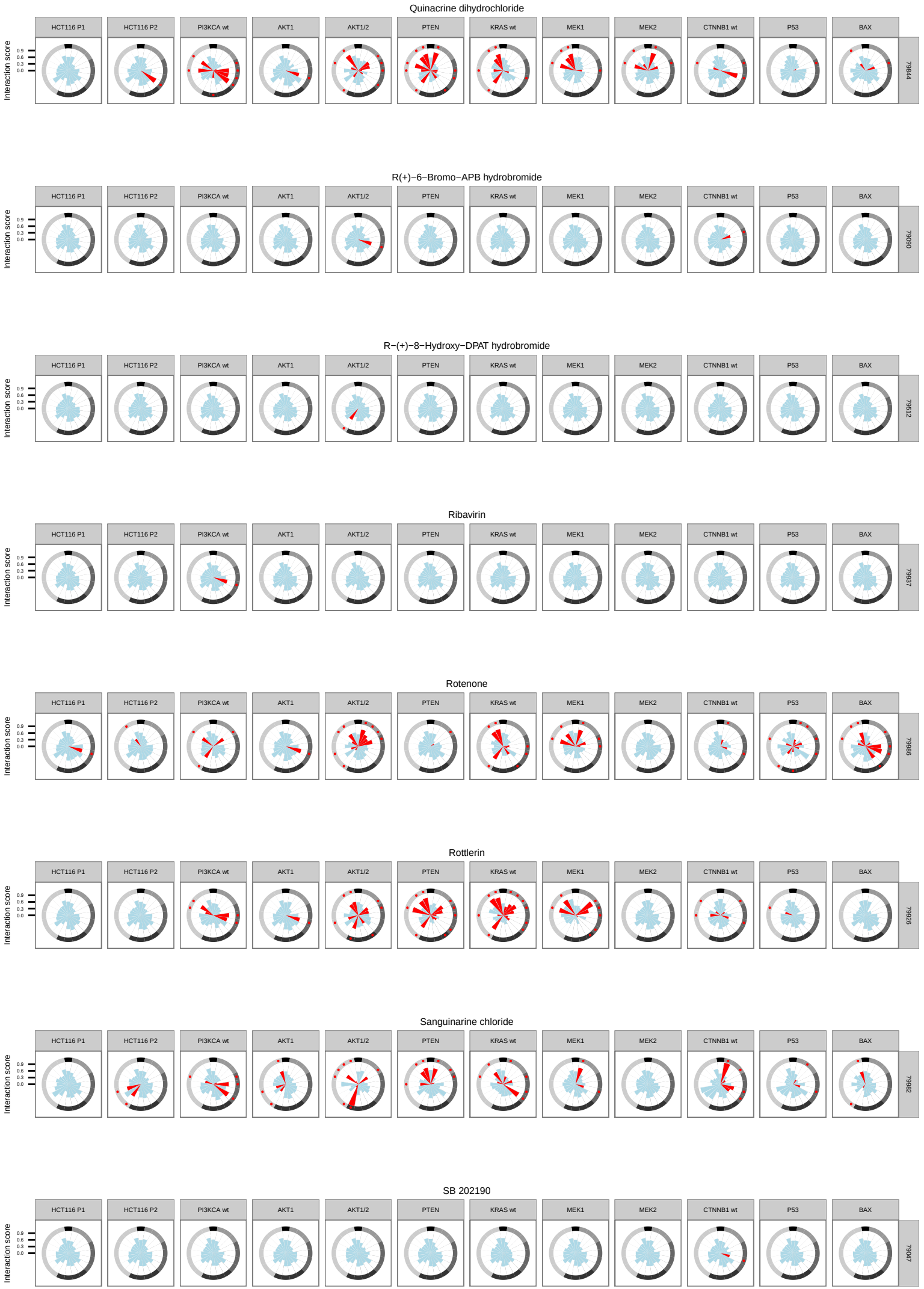
Quinacrine dihydrochloride
R(+)−6−Bromo−APB hydrobromide
R−(+)−8−Hydroxy−DPAT hydrobromide
Ribavirin
Rotenone
Rottlerin
Sanguinarine chloride
SB 202190
HCT116 P1
HCT116 P2
PI3KCA wt
AKT1
AKT1/2
PTEN
KRAS wt
MEK1
MEK2
CTNNB1 wt
P53
BAX
Interaction score
0.9
0.6
0.3
0.0
79844
79090
79512
79937
79986
79926
79982
79047

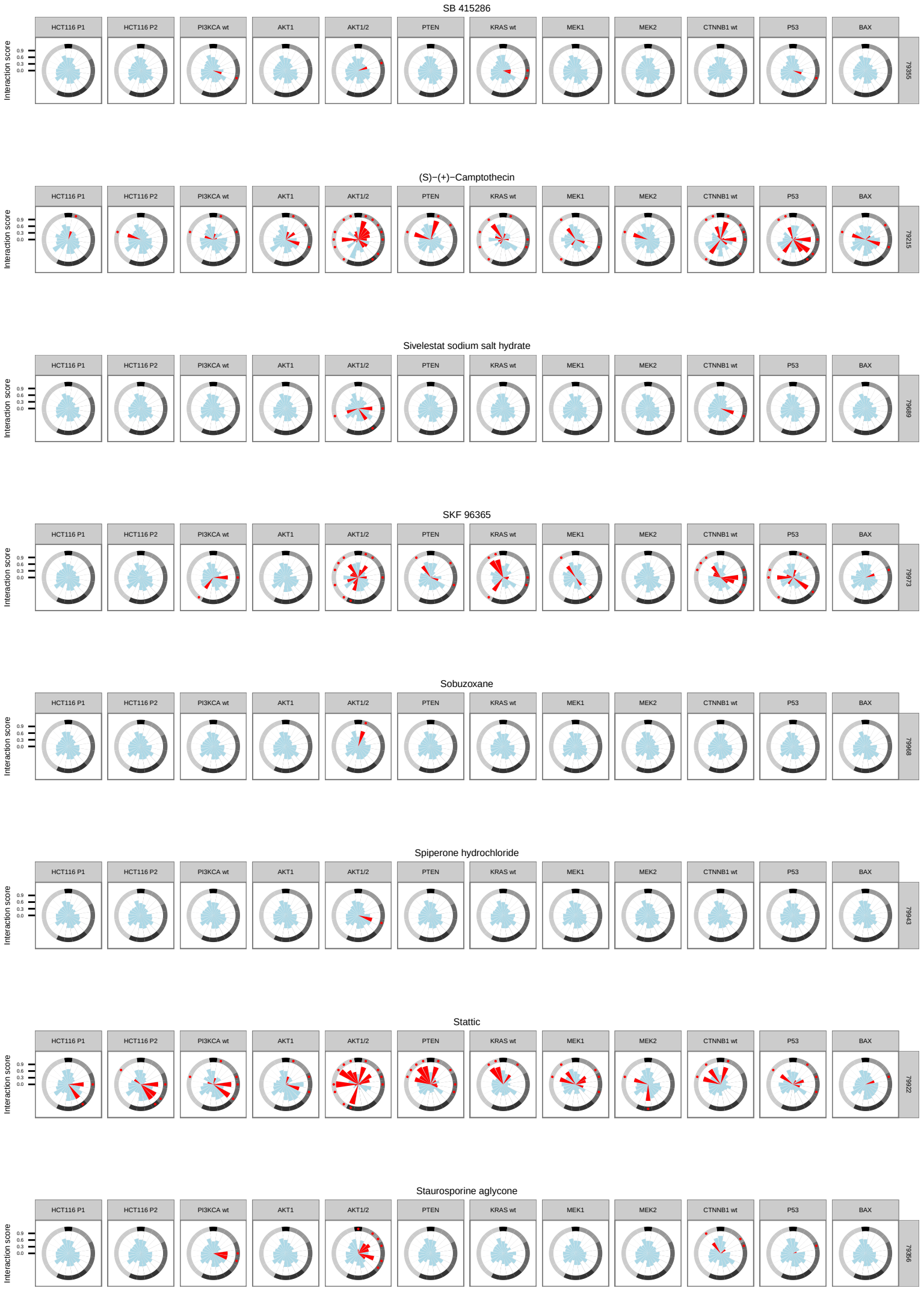
SB 415286
(S)−(+)−Camptothecin
Sivelestat sodium salt hydrate
SKF 96365
Sobuzoxane
Spiperone hydrochloride
Stattic
Staurosporine aglycone
HCT116 P1
HCT116 P2
PI3KCA wt
AKT1
AKT1/2
PTEN
KRAS wt
MEK1
MEK2
CTNNB1 wt
P53
BAX
Interaction score
0.9
0.6
0.3
0.0
79355
79215
79689
79973
79968
79943
79922
79356

SU 5416

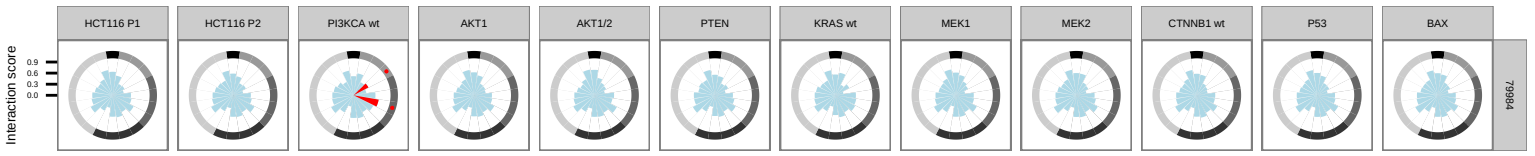

(−)−Sulpiride

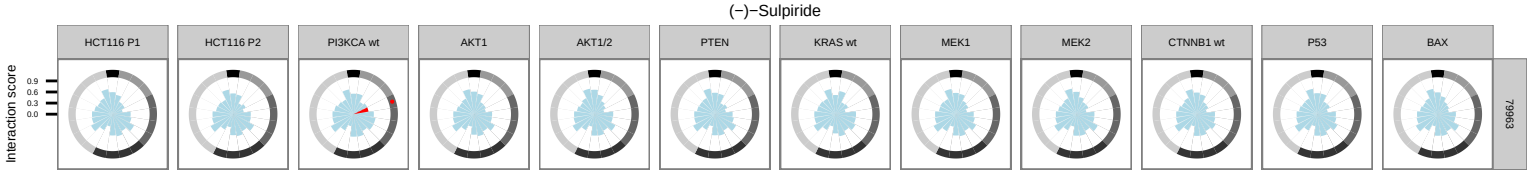

Supercinnamaldehyde

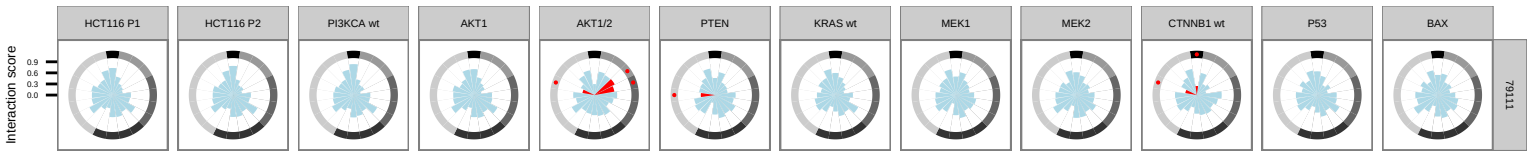

Taxol

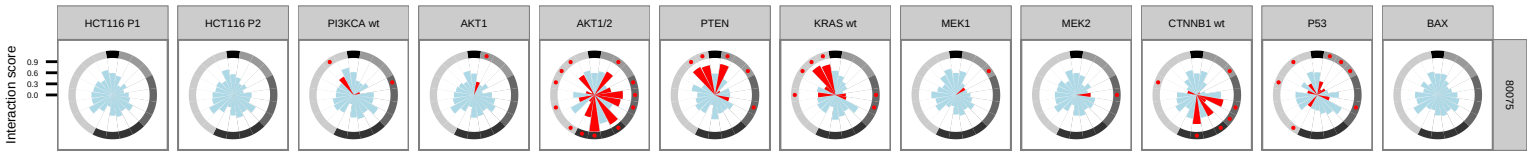

TBBz

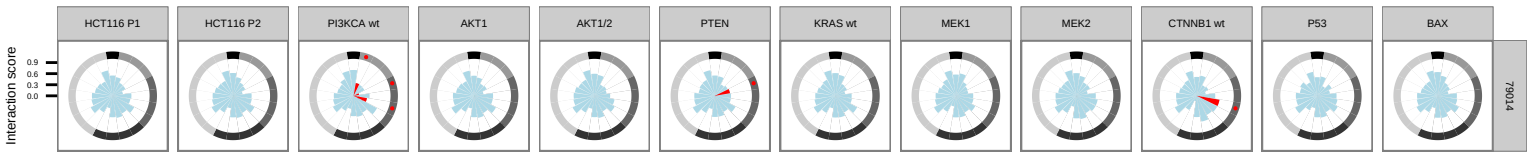

Terfenadine

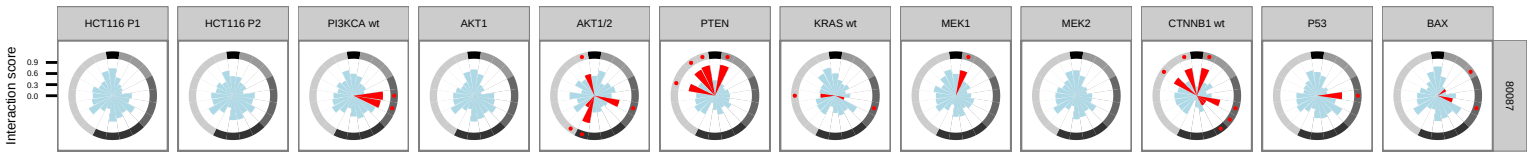

Tetraethylthiuram disulfide

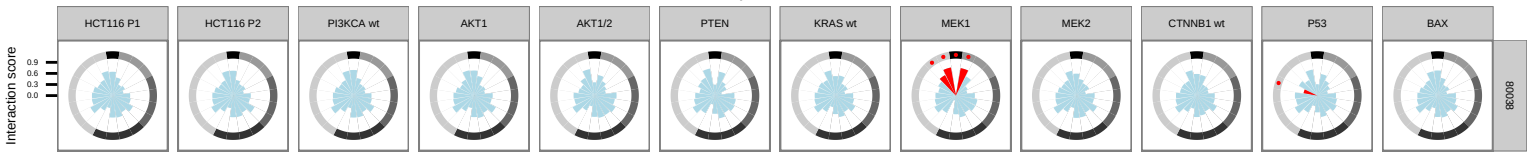

Thapsigargin

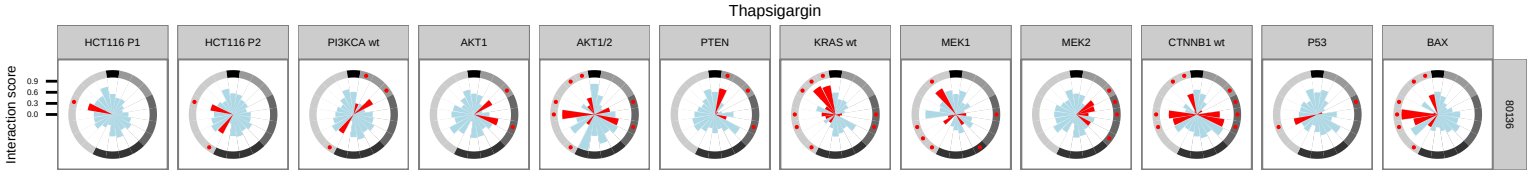

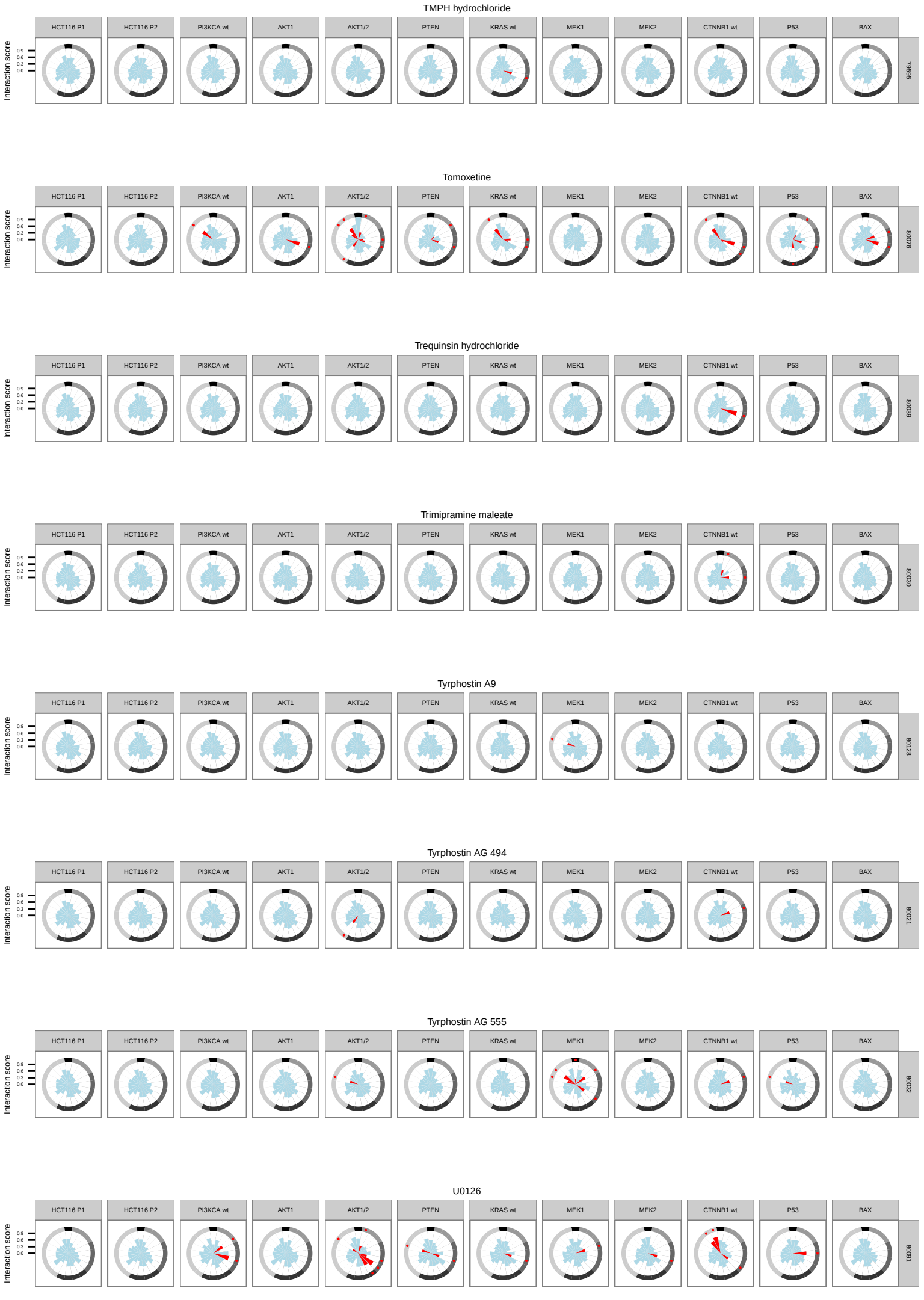
TMPH hydrochloride
Tomoxetine
Trequinsin hydrochloride
Trimipramine maleate
Tyrphostin A9
Tyrphostin AG 494
Tyrphostin AG 555
U0126
HCT116 P1
HCT116 P2
PI3KCA wt
AKT1
AKT1/2
PTEN
KRAS wt
MEK1
MEK2
CTNNB1 wt
P53
BAX
Interaction score
0.9
0.6
0.3
0.0
79595
80076
80039
80030
80128
80021
80032
80091

U−74389G maleate

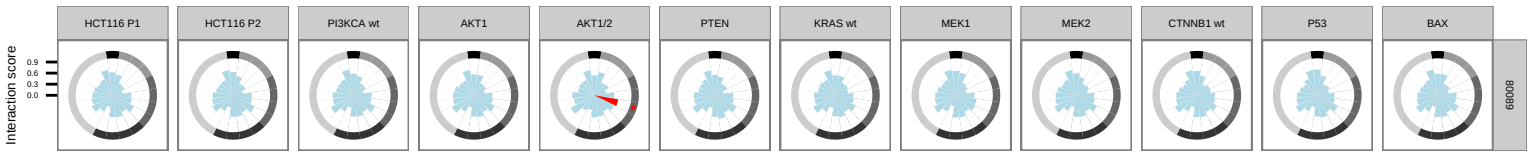

(+−)−Vesamicol hydrochloride

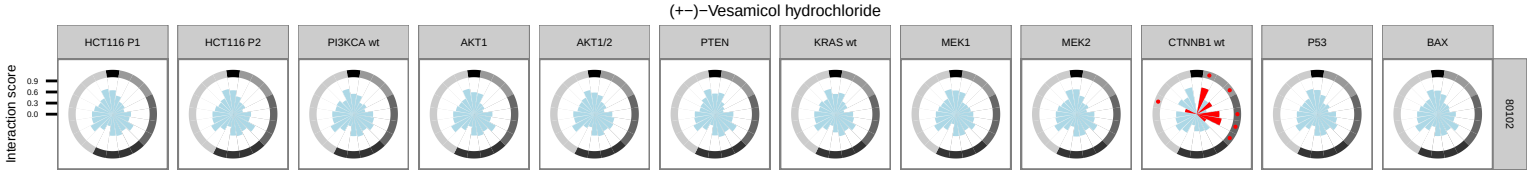

Vinblastine sulfate salt

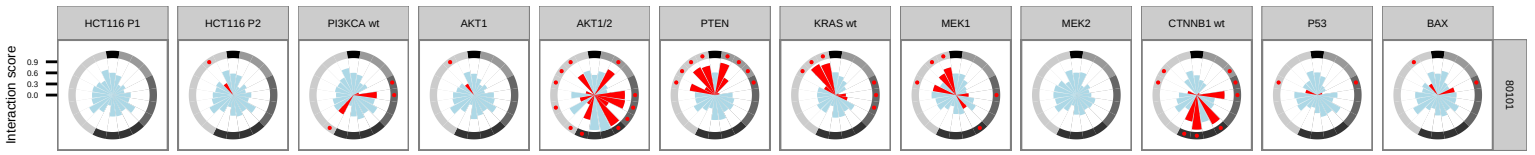

Vincristine sulfate

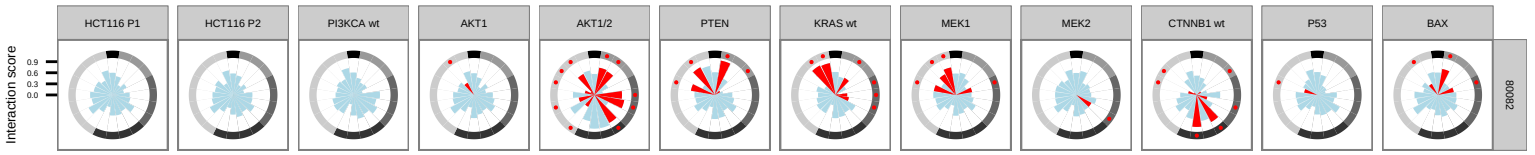

WIN 62,577

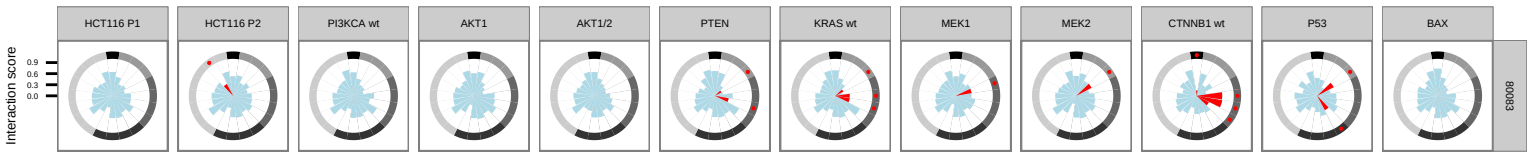

Wortmannin from Penicillium funiculosum

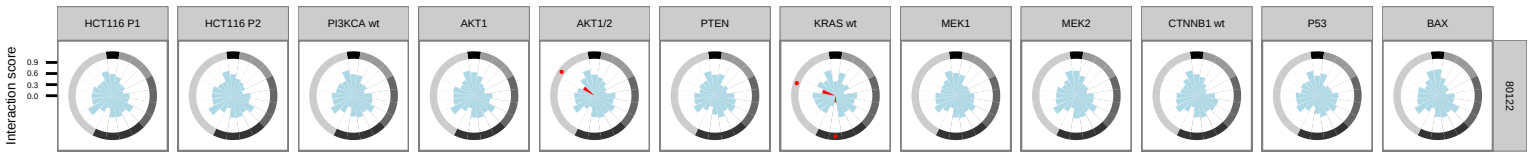

Y−27632 dihydrochloride

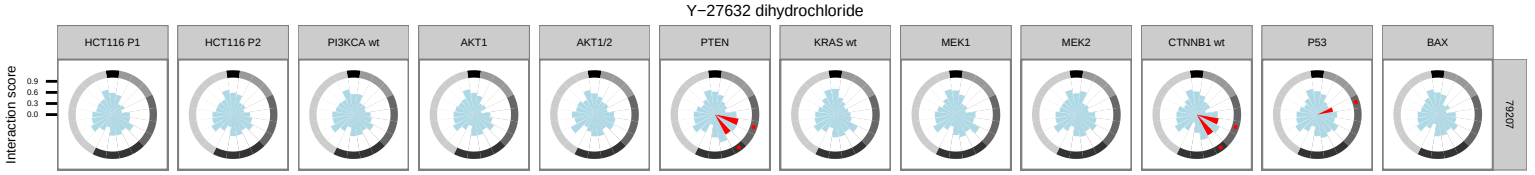

YC−1

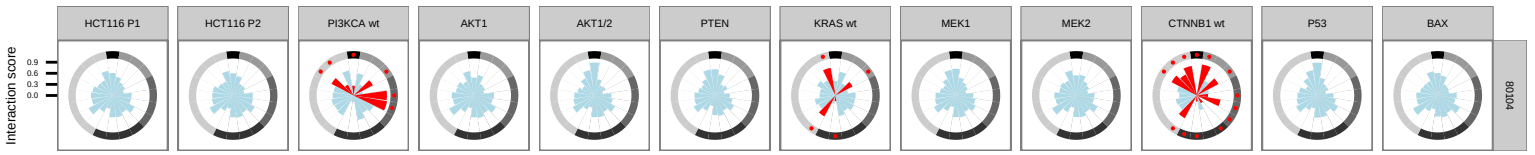

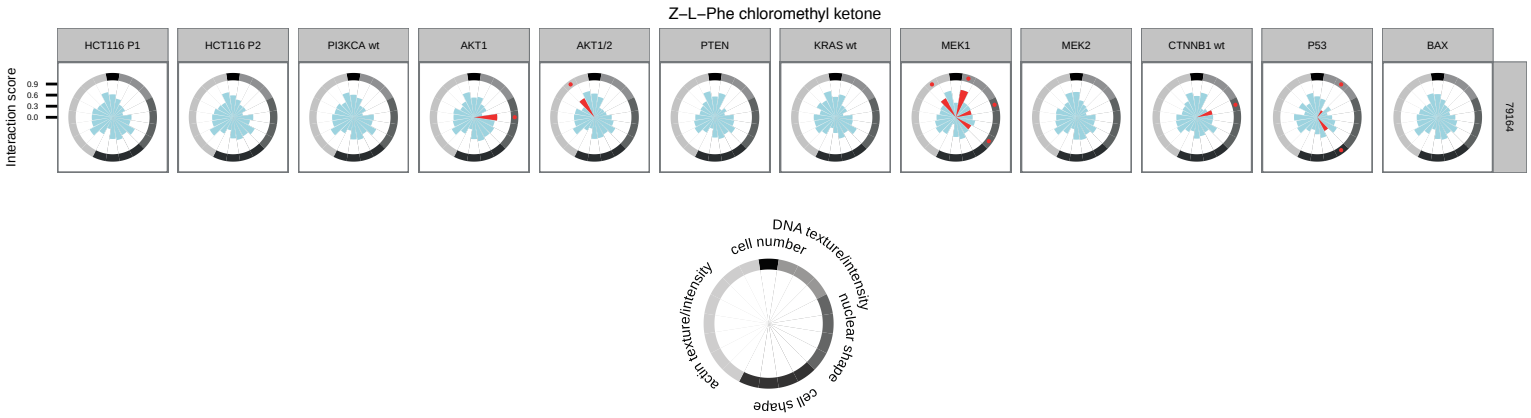

Appendix Figure S4. Significant multiparametric chemical-genetic interactions.

Chemical-genetic interactions were calculated for all 20 phenotypic features as described. A total of 193 compounds revealed significant interactions and their respective interaction spectra are plotted alphabetically.
Interactions are scaled from 0-1. * FDR < 0.01, highlighted in red.

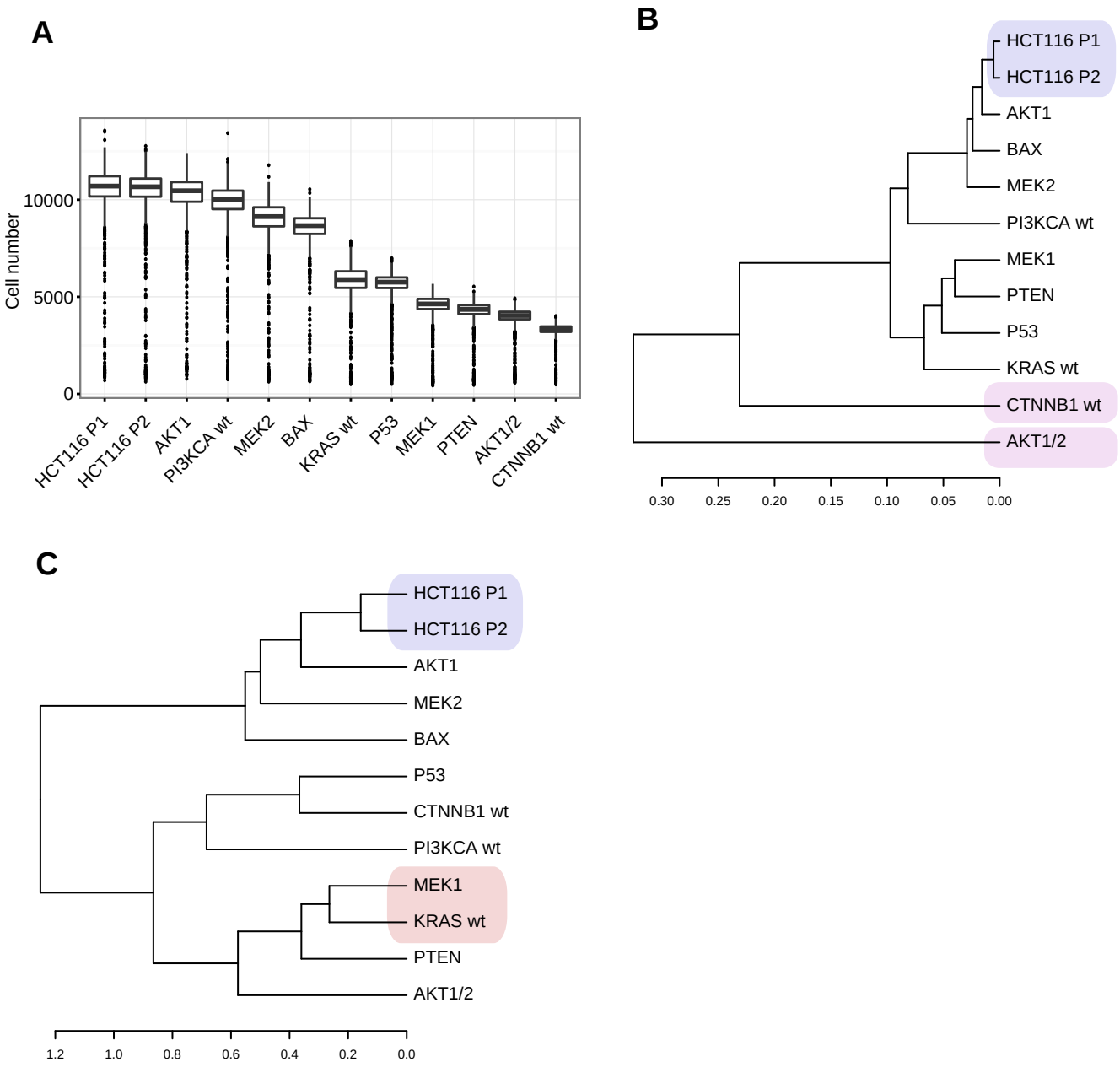

Appendix Figure S5. Strong main effects of gene KO and associations of isogenic cell lines.
A Cell number for each isogenic cell line tested after 48h growth under control conditions (DMSO treatment). Particular isogenic cell lines display a pronounced phenotypic effect, i.e. impaired proliferation as compared to parental HCT116 cells.
B Unsupervised clustering of isogenic cell lines based on their 20-feature phenotype signature reveals that the parental HCT116 cell lines from two different sources cluster tightly together. CTNNB1 wt cells and AKT1/2 KO cells cluster apart from the other cell lines, indicating that the KO of respective genes induces strong phenotypic main effects.
C Unsupervised clustering of the phenotypic chemical-genetic interaction profiles for all drugs on all 20 phenotypic features reveals that the parental HCT116 cell lines from two different sources cluster tightly together. KRAS wt cluster together with MEK1 KO and not with MEK2 KO cells, indicating the key role of MEK1 in KRAS signaling.

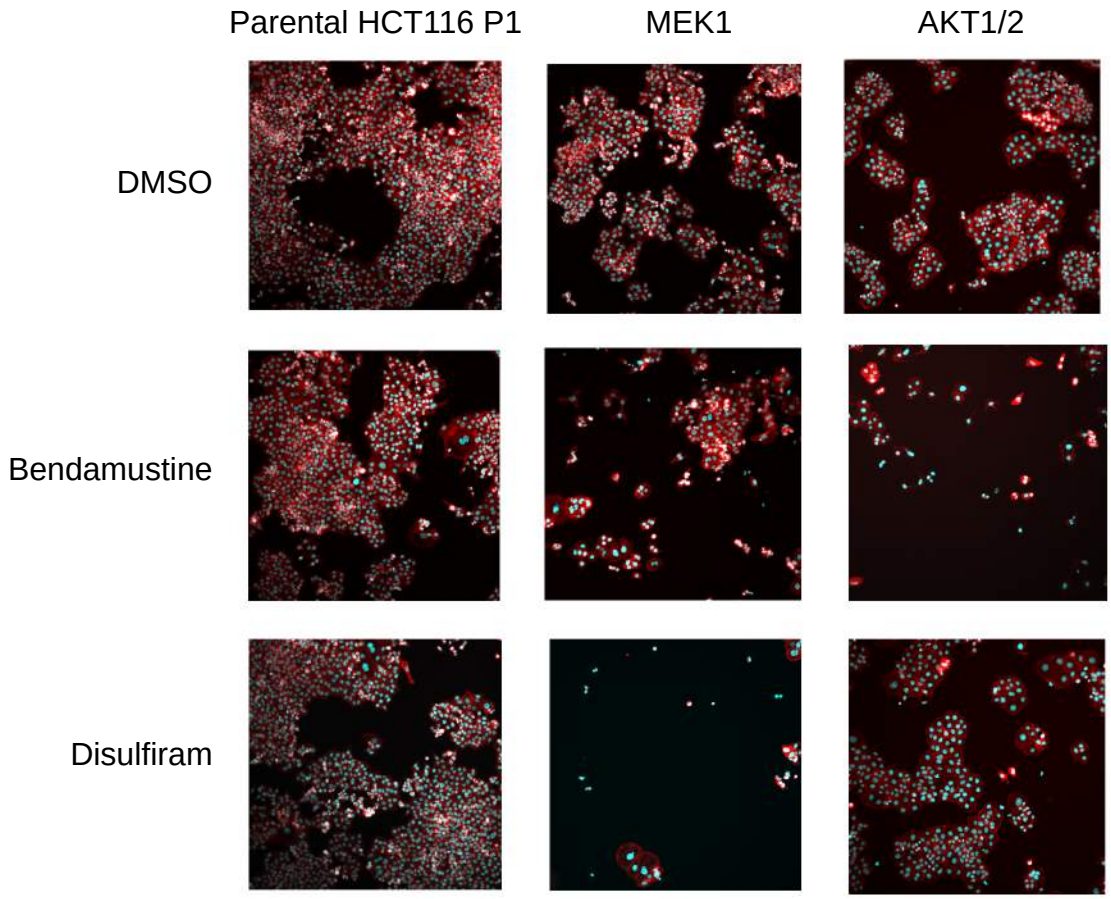

Appendix Figure S6. Synthetic lethal pharmacogenetic interactions.
Bendamustine specifically impaired the growth of AKT1/2 KO cells.
Disulfiram specifically impaired the growth of MEK1 KO cells.
Actin = red, DNA = cyan.

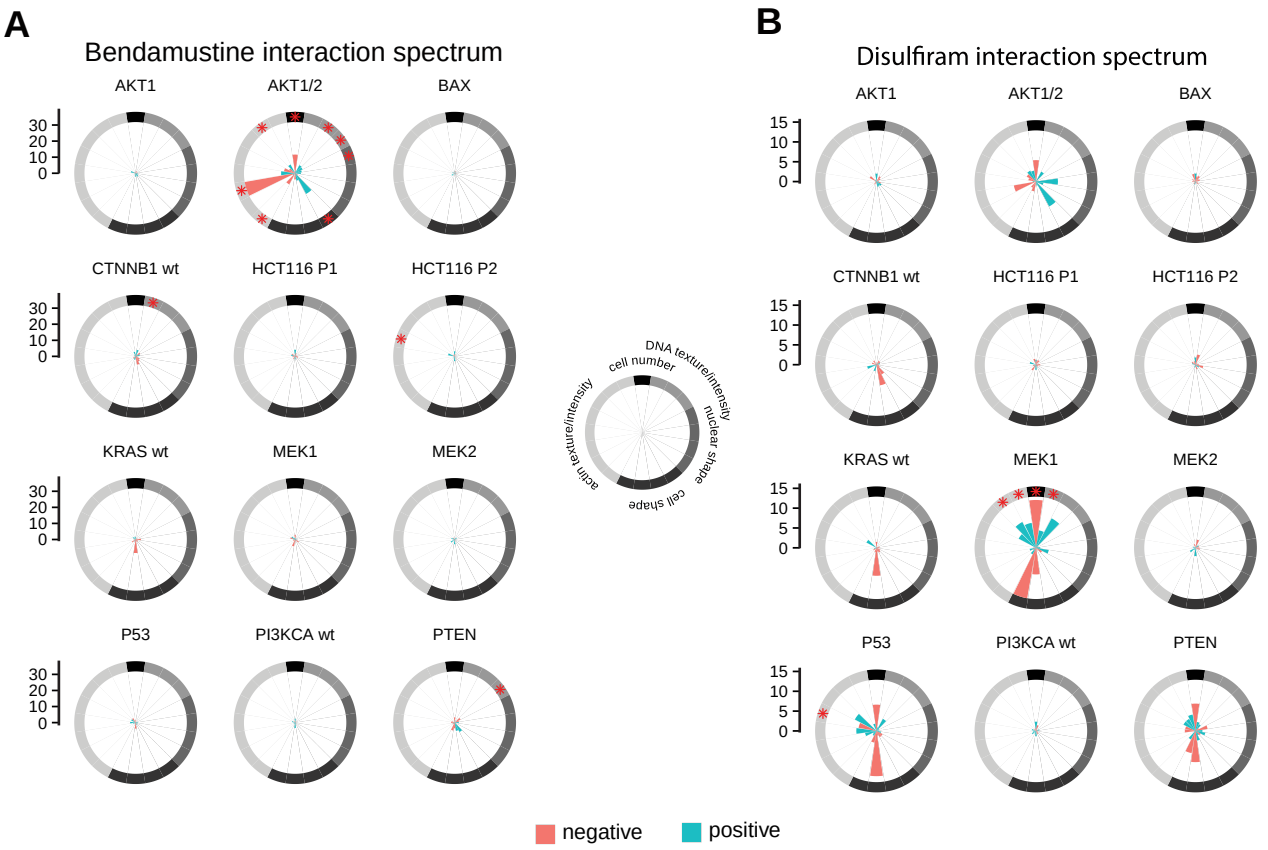

Appendix Figure S7. Bendamustine and disulfiram interaction spectrum.
A Bendamustine interaction spectrum. Bendamustine revealed chemical-genetic interactions across multiple phenotypic features including cell number in AKT1/2 double KO cells (highlighted in red).
B Disulfiram interaction spectrum. Disulfiram revealed chemical-genetic interactions across multiple phenotypic features, including cell number in MEK1 KO cells (highlighted in red). Phenotypic chemo-genomic interactions are shown unscaled which reveals that interactions are rare. Interactions are further categorized in positive and negative interactions according to the sign of interaction terms. * adjusted p-value < 0.01.

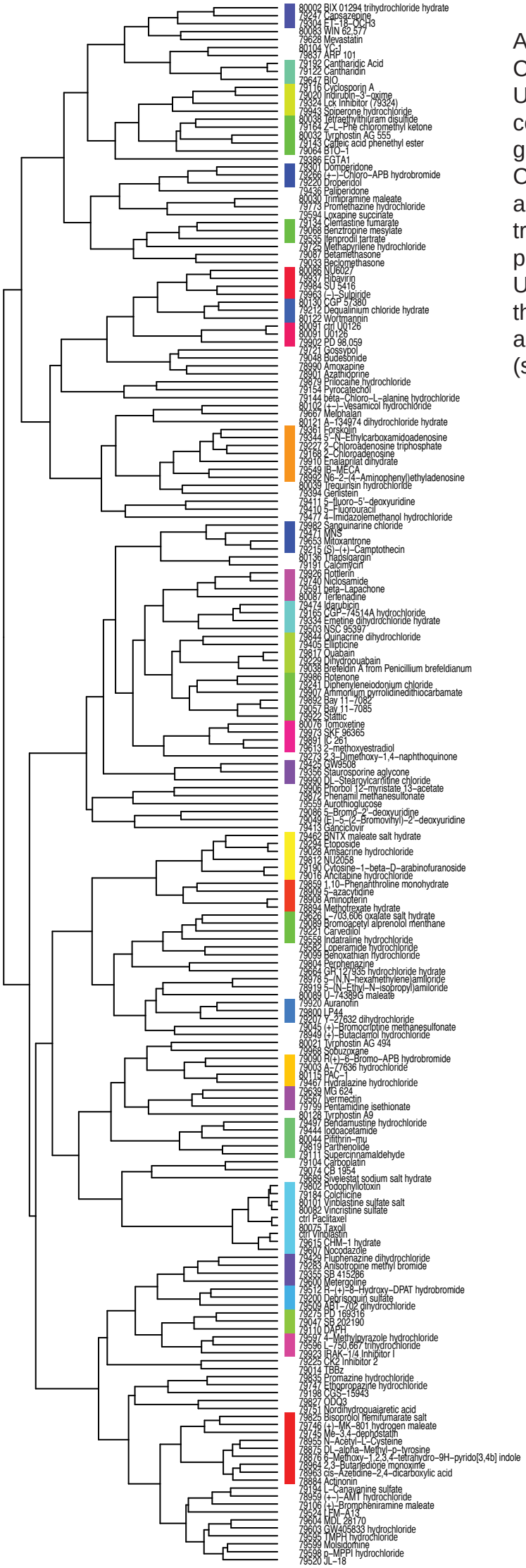

Appendix Figure S8.
Clustering of chemical-genetic interactions. Unsupervised clustering based on the correlation of interaction profiles of all genetic backgrounds for 20 phenotypic features. Color coding visualizes automated cluster analysis using a 0.6 height cutoff for the cluster tree and the inclusion of >2 and <10 drugs per cluster.
Unique drug identifiers for compounds in the LOPAC library as supplied by Sigma as well as compound names are depicted (see also Table EV1).

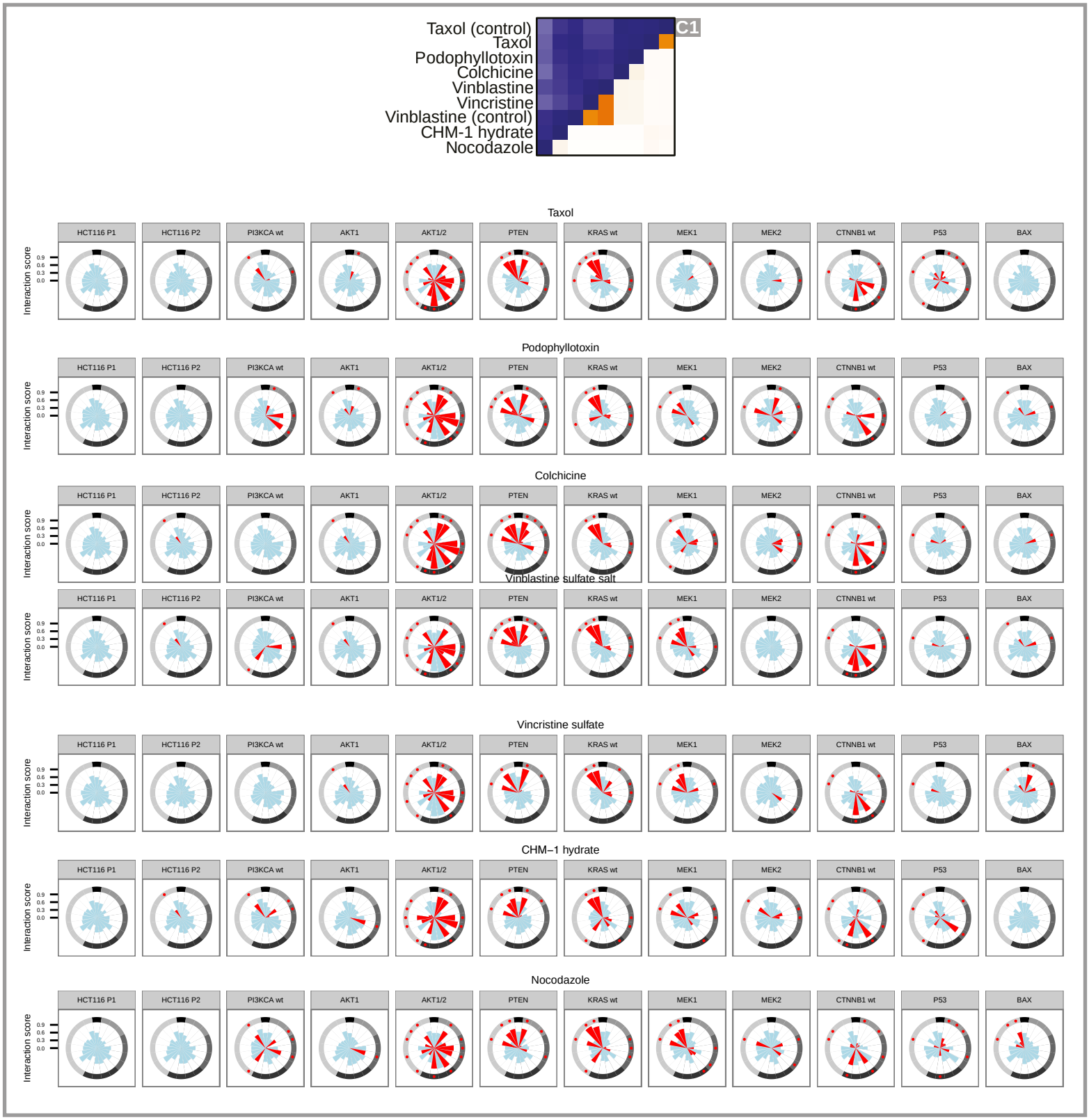
Taxol (control)
Taxol
Podophyllotoxin
Colchicine
Vinblastine
Vincristine
Vinblastine (control)
CHM-1 hydrate
Nocodazole
C1
Taxol
Podophyllotoxin
Colchicine
Vinblastine sulfate salt
Vincristine sulfate
CHM−1 hydrate
Nocodazole
HCT116 P1
HCT116 P2
PI3KCA wt
AKT1
AKT1/2
PTEN
KRAS wt
MEK1
MEK2
CTNNB1 wt
P53
BAX
Interaction score
0.9
0.6
0.3
0.0

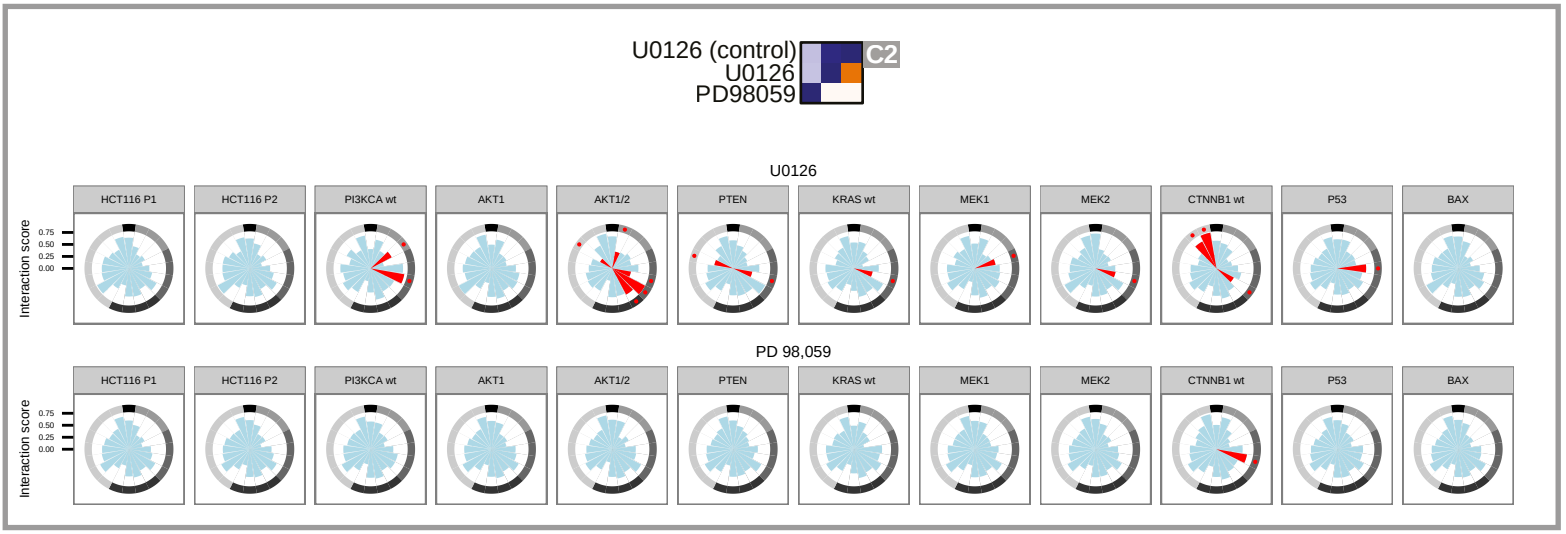
U0126 (control)
U0126
PD98059
C2
U0126
PD 98,059
HCT116 P1
HCT116 P2
PI3KCA wt
AKT1
AKT1/2
PTEN
KRAS wt
MEK1
MEK2
CTNNB1 wt
P53
BAX
Interaction score
0.75
0.50
0.25
0.00

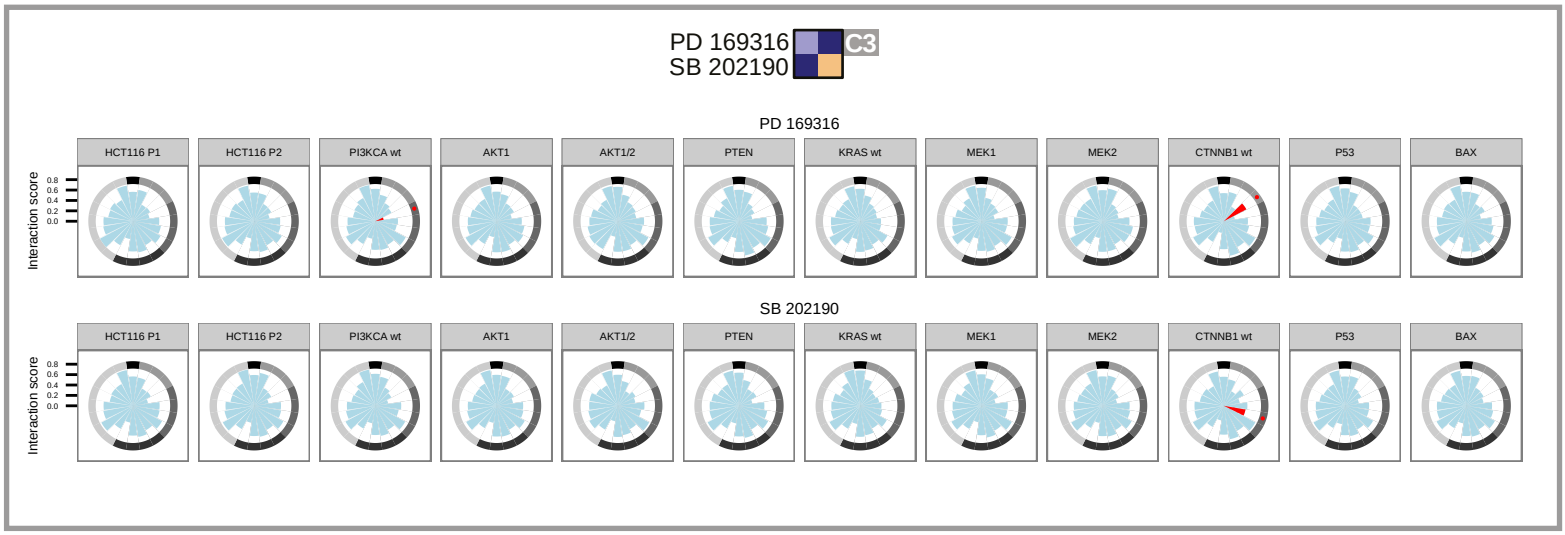
PD 169316
SB 202190
C3
PD 169316
SB 202190
HCT116 P1
HCT116 P2
PI3KCA wt
AKT1
AKT1/2
PTEN
KRAS wt
MEK1
MEK2
CTNNB1 wt
P53
BAX
Interaction score

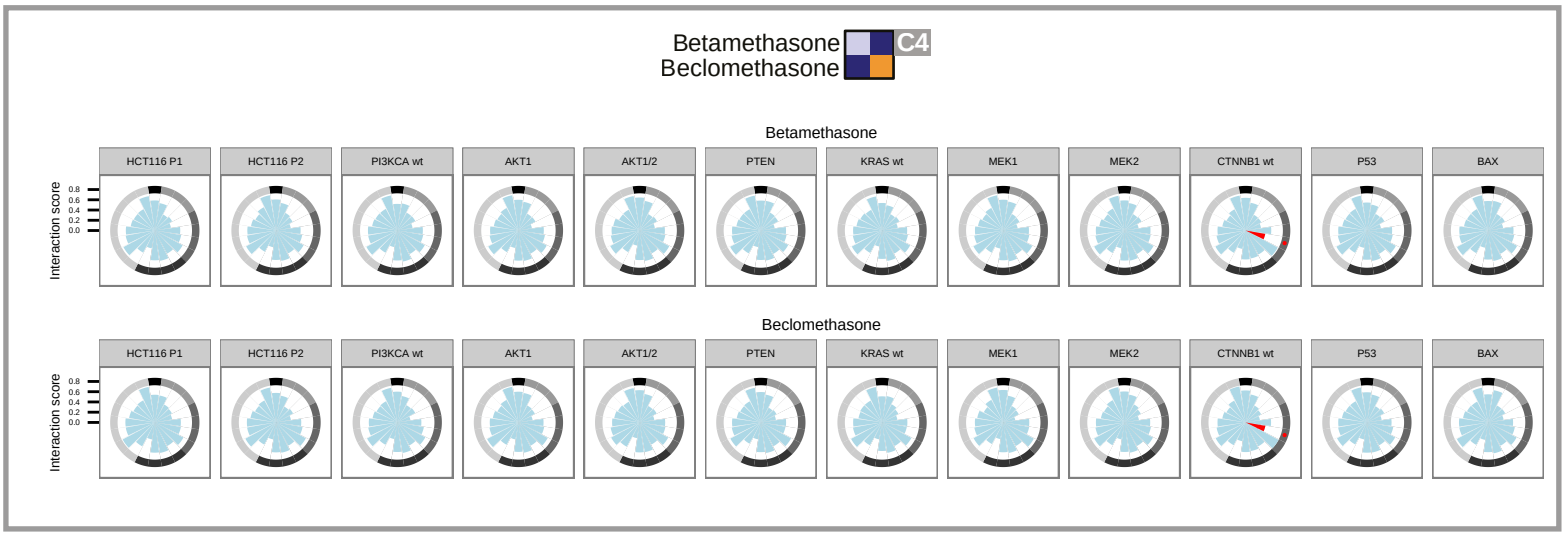
Betamethasone
Beclomethasone
C4
Betamethasone
Beclomethasone
HCT116 P1
HCT116 P2
PI3KCA wt
AKT1
AKT1/2
PTEN
KRAS wt
MEK1
MEK2
CTNNB1 wt
P53
BAX
Interaction score

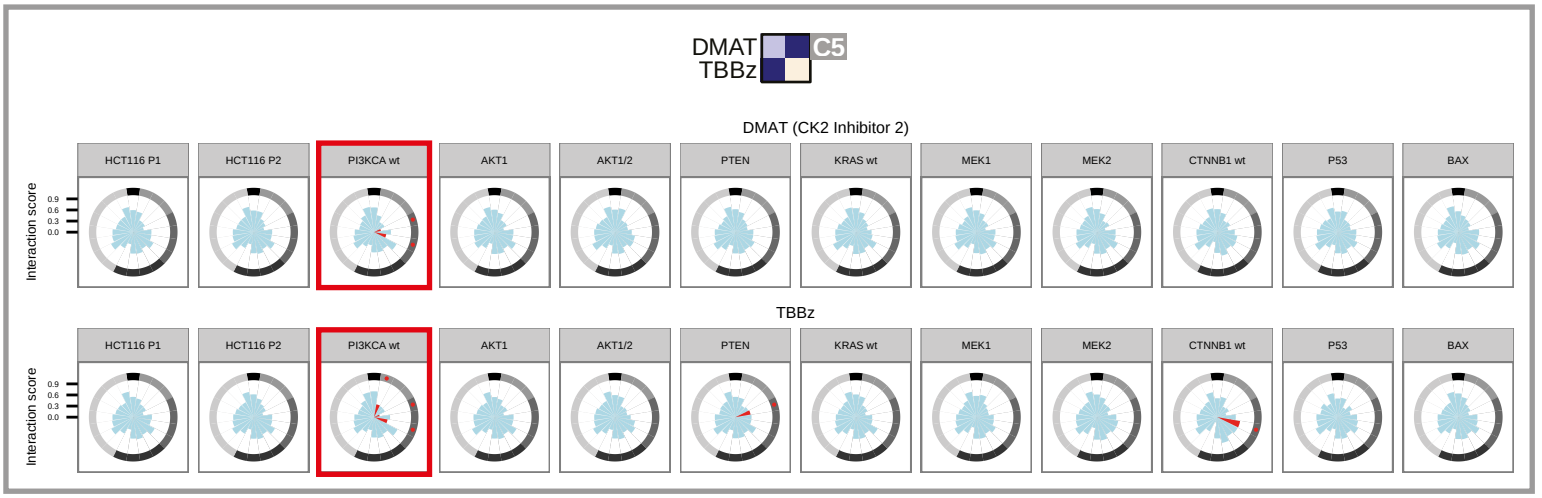
DMAT
TBBz
C5
DMAT (CK2 Inhibitor 2)
TBBz
HCT116 P1
HCT116 P2
PI3KCA wt
AKT1
AKT1/2
PTEN
KRAS wt
MEK1
MEK2
CTNNB1 wt
P53
BAX
Interaction score

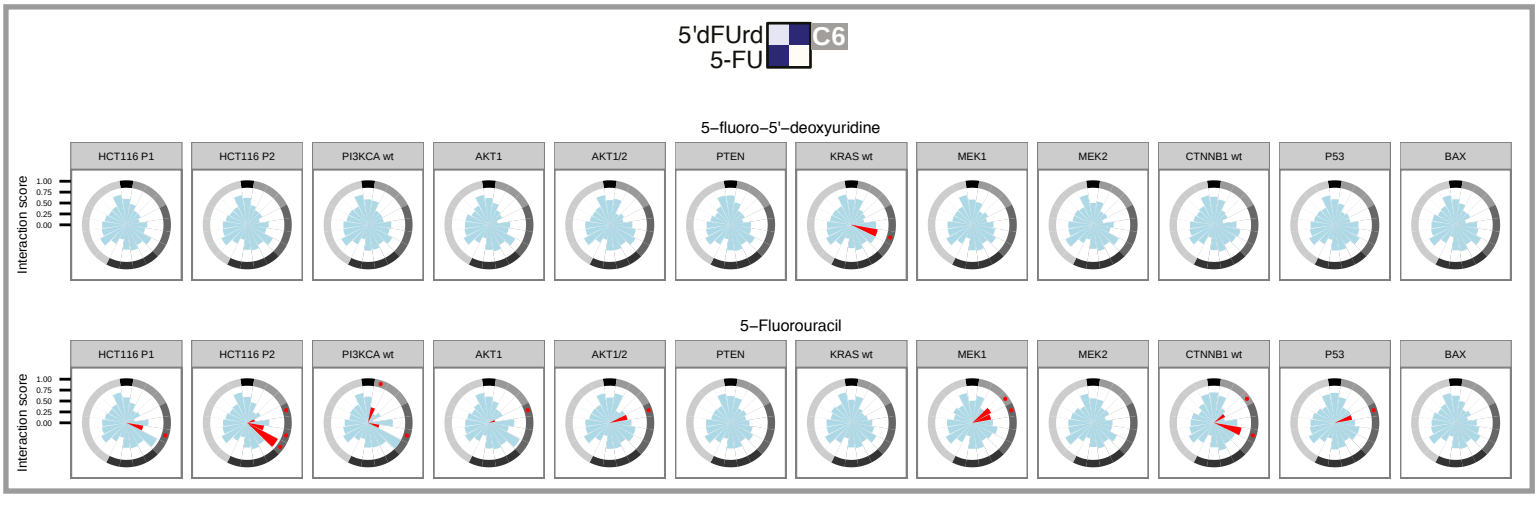
5'dFUrd
5-FU
C6
5−fluoro−5'−deoxyuridine
5−Fluorouracil
HCT116 P1
HCT116 P2
PI3KCA wt
AKT1
AKT1/2
PTEN
KRAS wt
MEK1
MEK2
CTNNB1 wt
P53
BAX
Interaction score

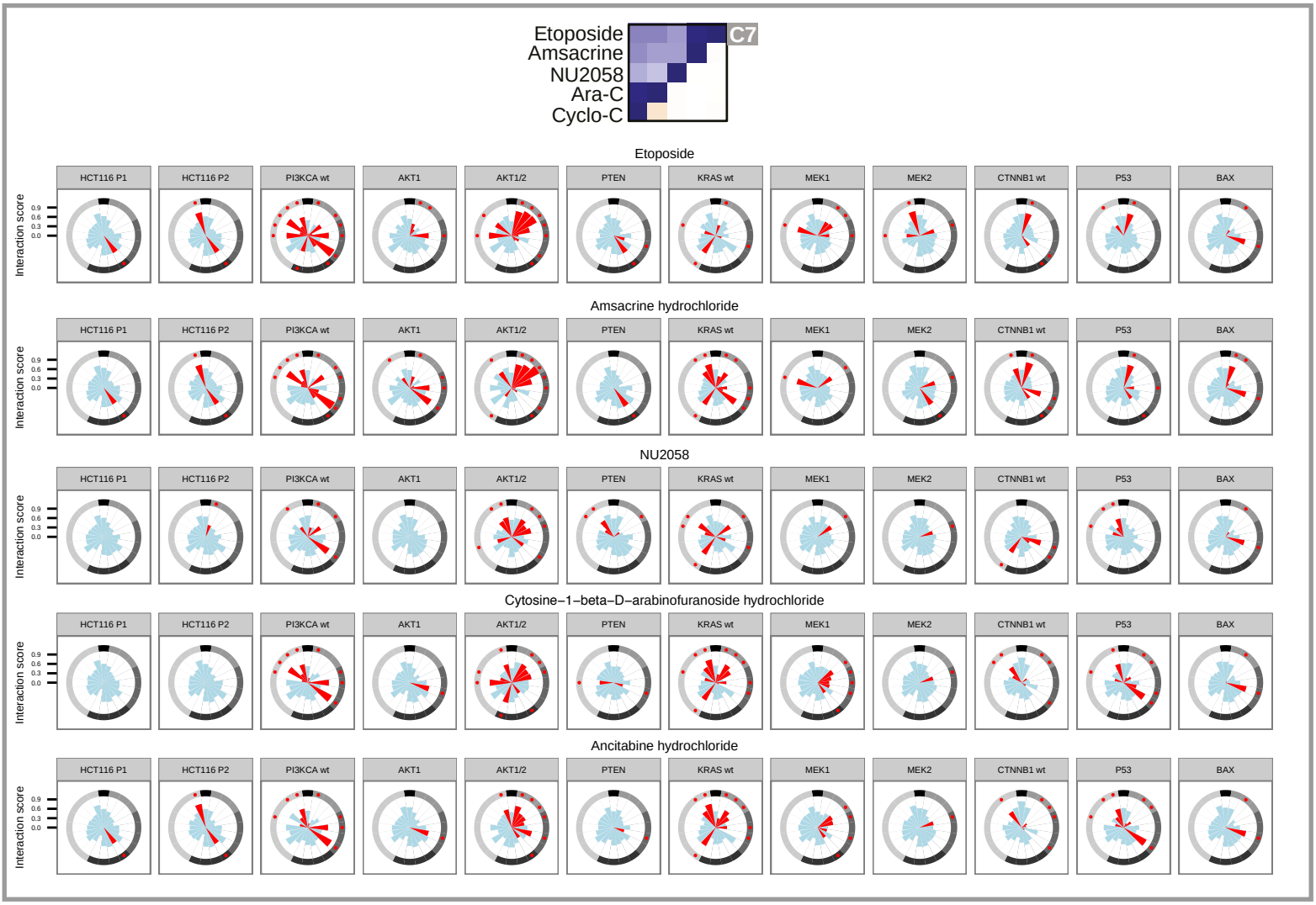
Etoposide
Amsacrine
NU2058
Ara-C
Cyclo-C
C7
Etoposide
Amsacrine hydrochloride
NU2058
Cytosine−1−beta−D−arabinofuranoside hydrochloride
Ancitabine hydrochloride
HCT116 P1
HCT116 P2
PI3KCA wt
AKT1
AKT1/2
PTEN
KRAS wt
MEK1
MEK2
CTNNB1 wt
P53
BAX
Interaction score
0.9
0.6
0.3
0.0

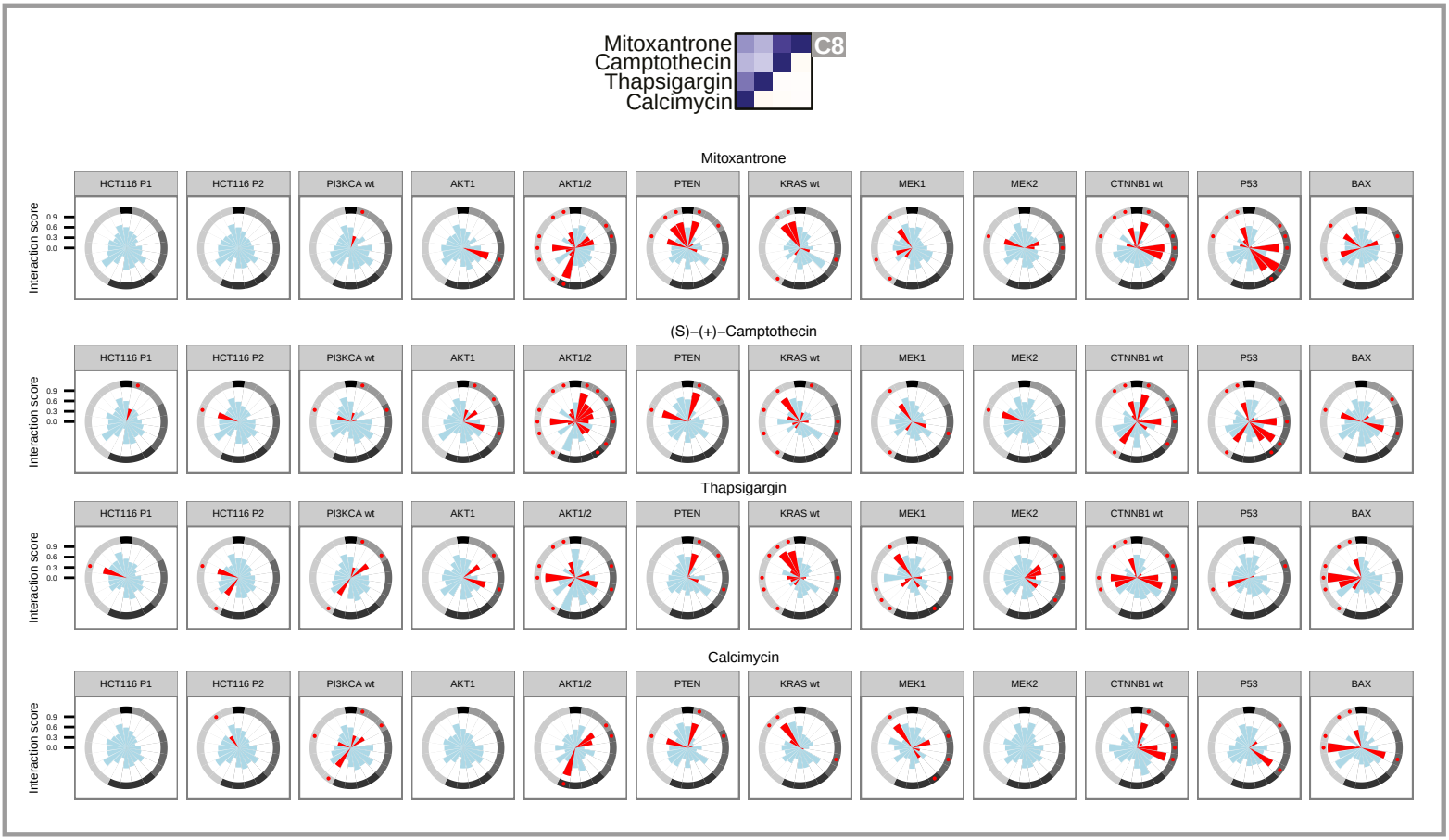
Mitoxantrone
Camptothecin
Thapsigargin
Calcimycin
C8
Mitoxantrone
(S)−(+)−Camptothecin
Thapsigargin
Calcimycin
HCT116 P1
HCT116 P2
PI3KCA wt
AKT1
AKT1/2
PTEN
KRAS wt
MEK1
MEK2
CTNNB1 wt
P53
BAX
Interaction score
0.9
0.6
0.3
0.0

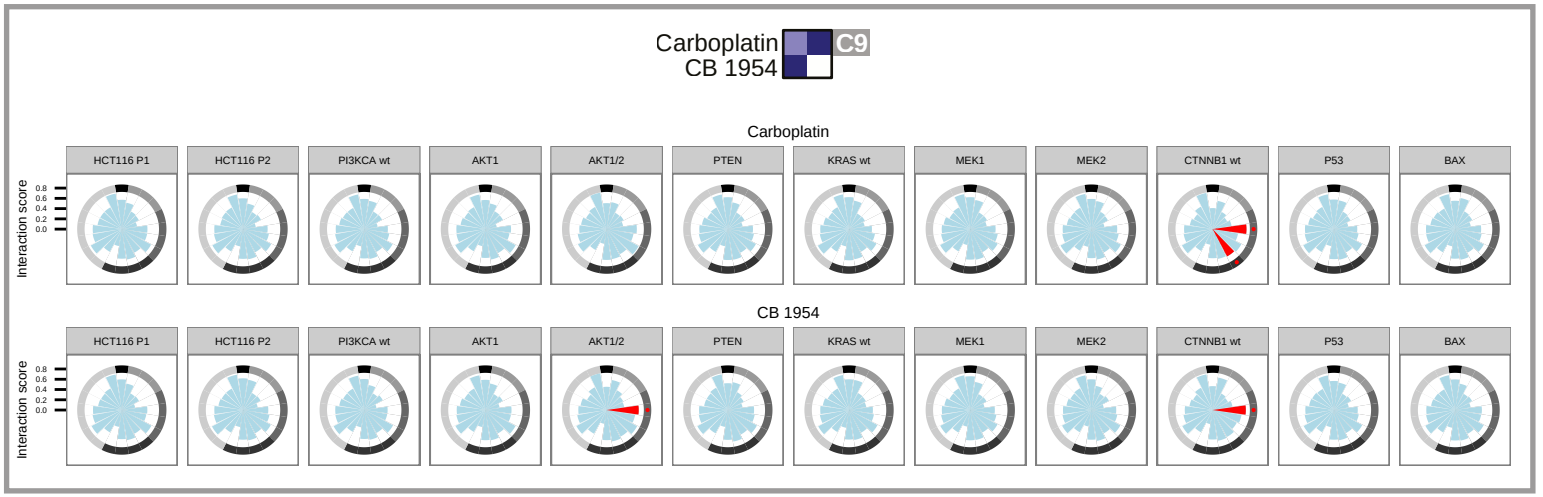
Carboplatin
CB 1954
C9
Carboplatin
CB 1954
HCT116 P1
HCT116 P2
PI3KCA wt
AKT1
AKT1/2
PTEN
KRAS wt
MEK1
MEK2
CTNNB1 wt
P53
BAX
Interaction score

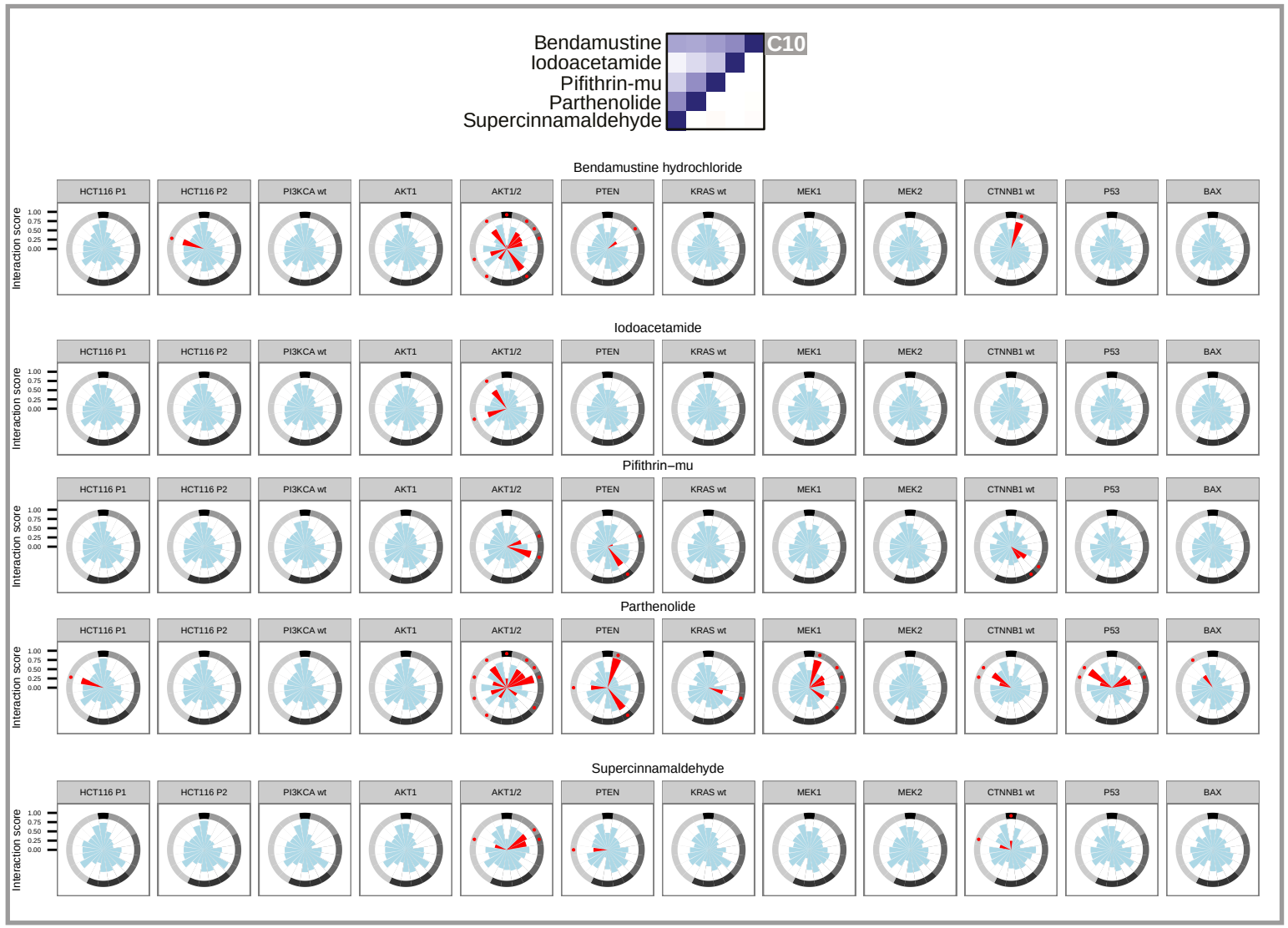
Bendamustine
Iodoacetamide
Pifithrin-mu
Parthenolide
Supercinnamaldehyde
C10
Bendamustine hydrochloride
Iodoacetamide
Pifithrin−mu
Parthenolide
Supercinnamaldehyde
HCT116 P1
HCT116 P2
PI3KCA wt
AKT1
AKT1/2
PTEN
KRAS wt
MEK1
MEK2
CTNNB1 wt
P53
BAX
Interaction score

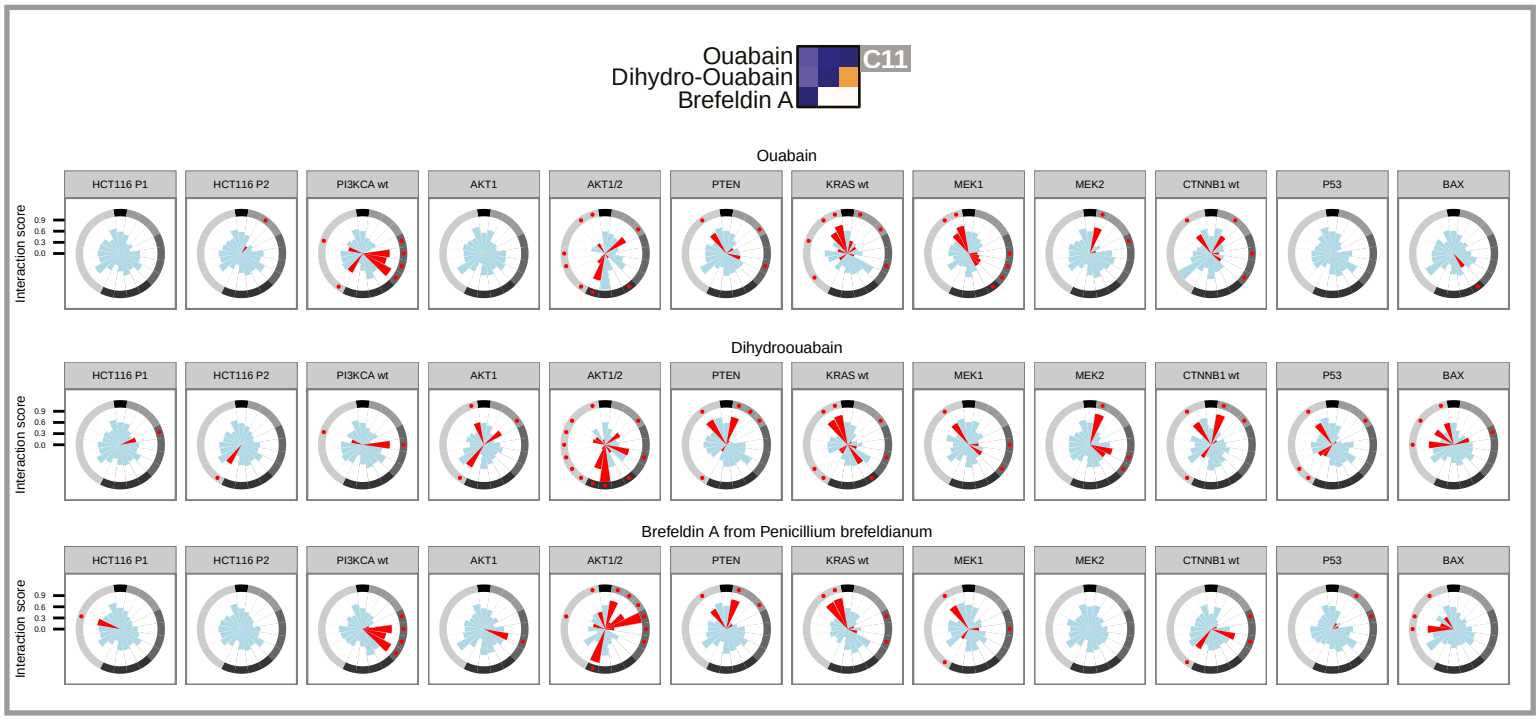
Ouabain
Dihydro-Ouabain
Brefeldin A
C11
Ouabain
Dihydroouabain
Brefeldin A from Penicillium brefeldianum
HCT116 P1
HCT116 P2
PI3KCA wt
AKT1
AKT1/2
PTEN
KRAS wt
MEK1
MEK2
CTNNB1 wt
P53
BAX
Interaction score
0.9
0.6
0.3
0.0

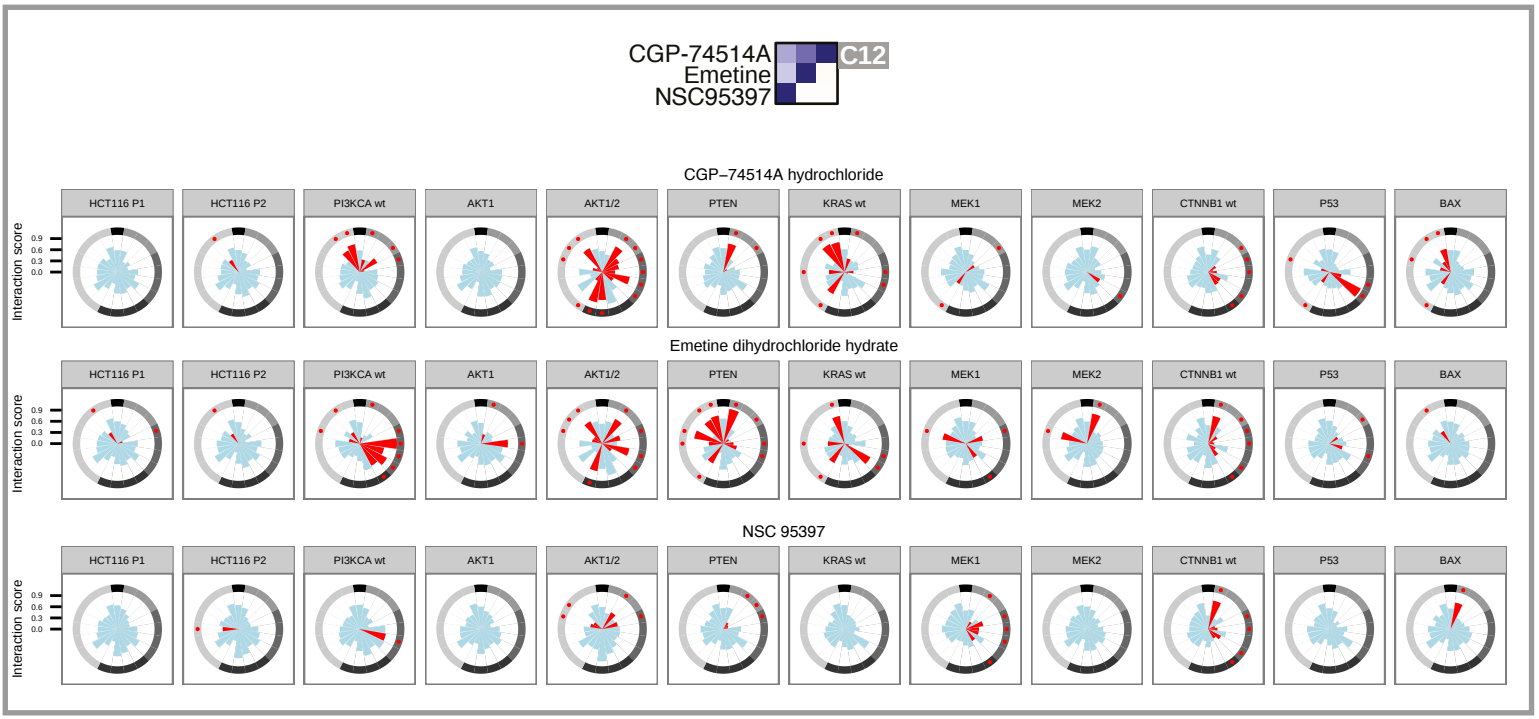
CGP-74514A
Emetine
NSC95397
C12
CGP−74514A hydrochloride
Emetine dihydrochloride hydrate
NSC 95397
HCT116 P1
HCT116 P2
PI3KCA wt
AKT1
AKT1/2
PTEN
KRAS wt
MEK1
MEK2
CTNNB1 wt
P53
BAX
Interaction score
0.9
0.6
0.3
0.0

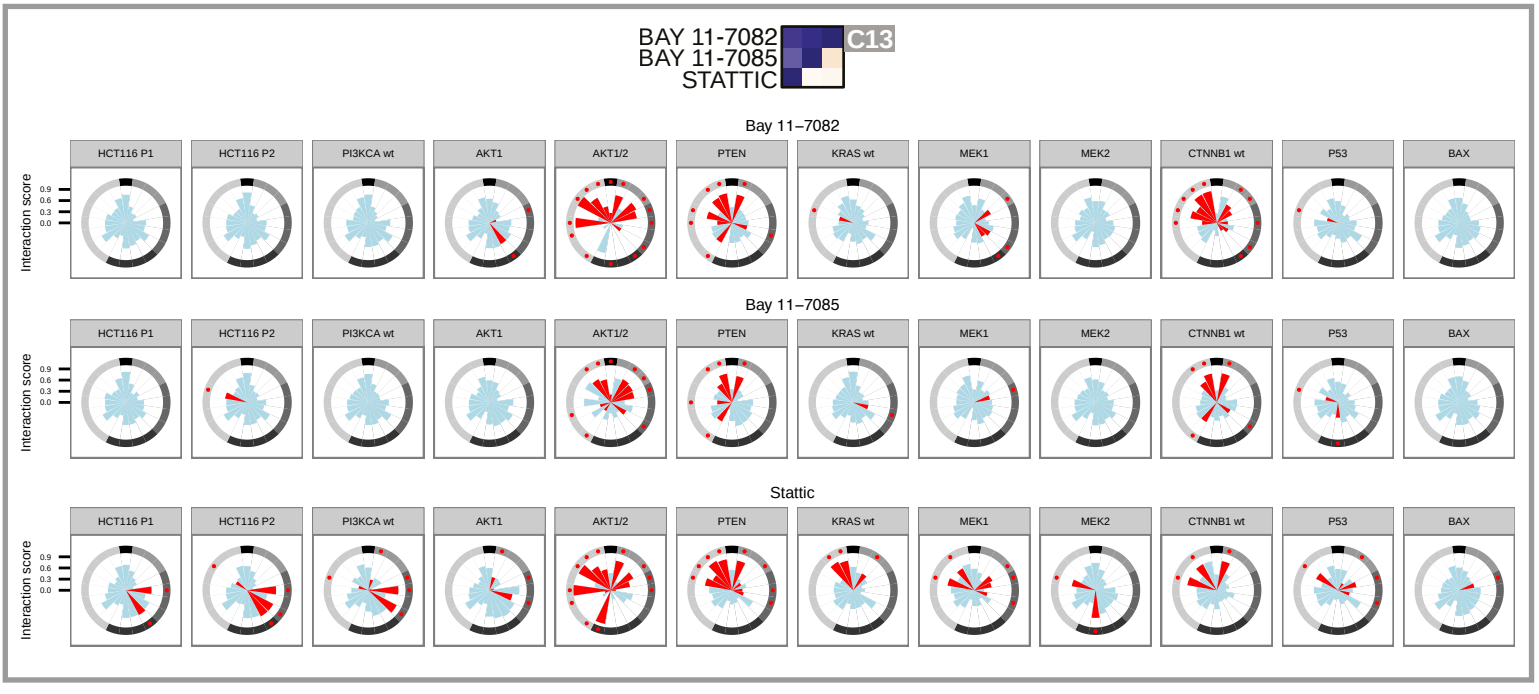
BAY 11-7082
BAY 11-7085
STATTIC
C13
Bay 11−7082
Bay 11−7085
Stattic
HCT116 P1
HCT116 P2
PI3KCA wt
AKT1
AKT1/2
PTEN
KRAS wt
MEK1
MEK2
CTNNB1 wt
P53
BAX
Interaction score
0.9
0.6
0.3
0.0

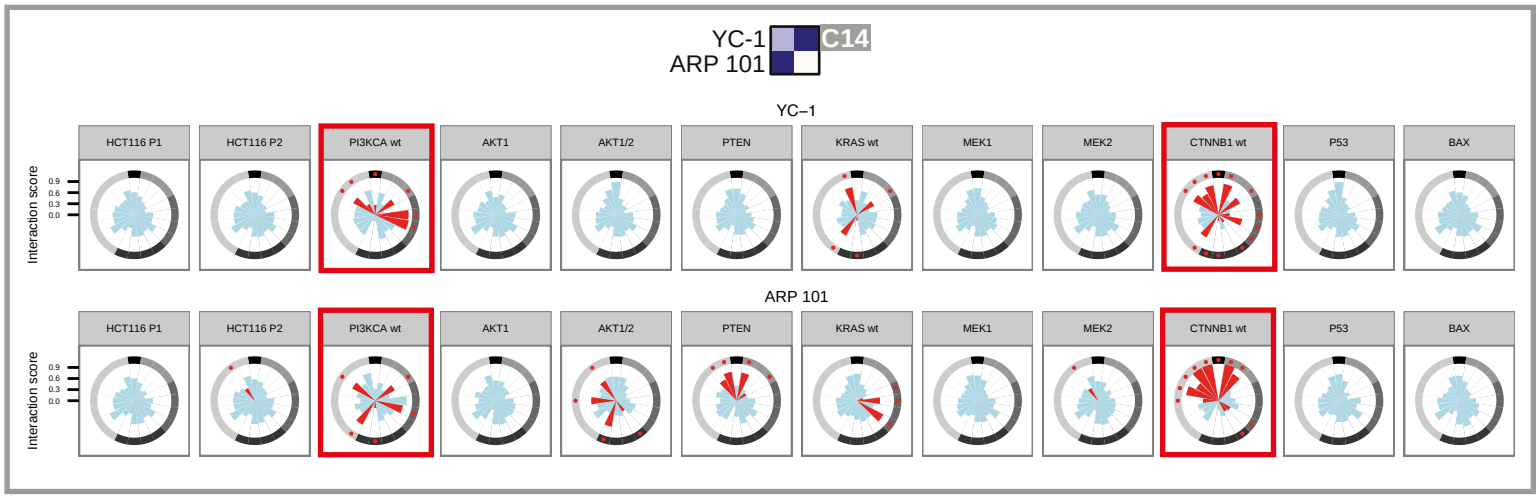
YC-1
ARP 101
C14
YC−1
ARP 101
Interaction score
HCT116 P1
HCT116 P2
PI3KCA wt
AKT1
AKT1/2
PTEN
KRAS wt
MEK1
MEK2
CTNNB1 wt
P53
BAX

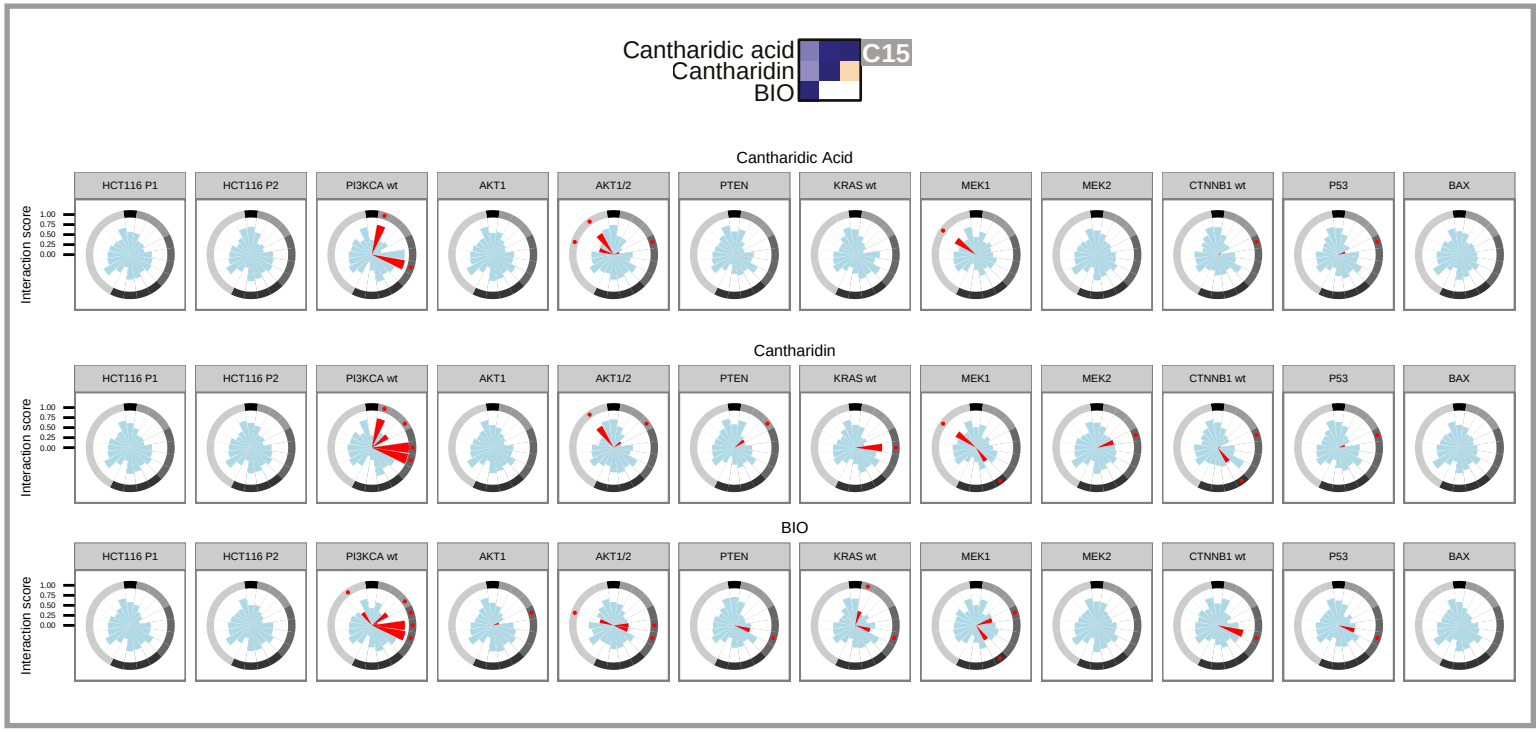
Cantharidic acid
Cantharidin
BIO
C15
Cantharidic Acid
Cantharidin
BIO
Interaction score
HCT116 P1
HCT116 P2
PI3KCA wt
AKT1
AKT1/2
PTEN
KRAS wt
MEK1
MEK2
CTNNB1 wt
P53
BAX

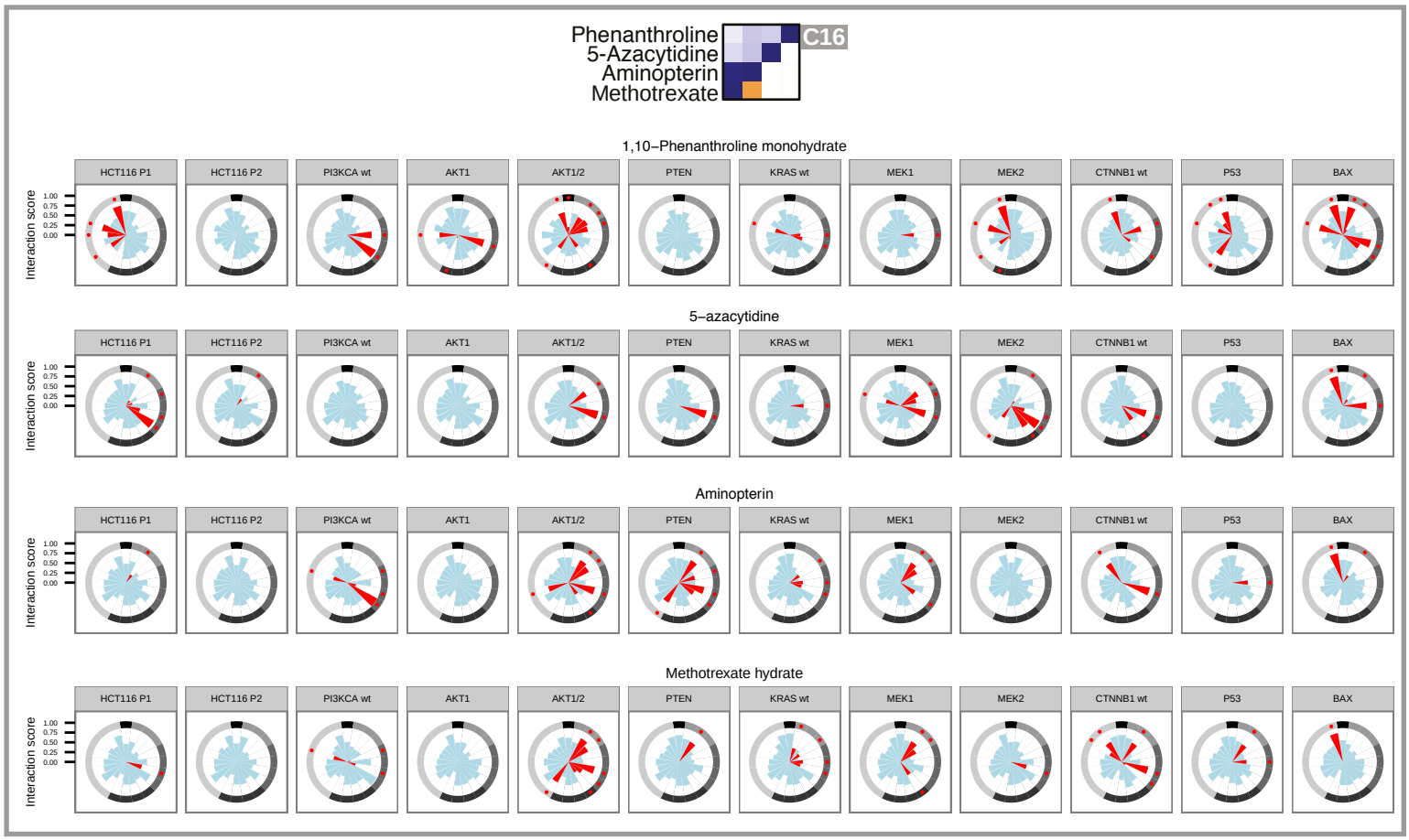
Phenanthroline
5-Azacytidine
Aminopterin
Methotrexate
C16
1,10−Phenanthroline monohydrate
5−azacytidine
Aminopterin
Methotrexate hydrate
Interaction score
HCT116 P1
HCT116 P2
PI3KCA wt
AKT1
AKT1/2
PTEN
KRAS wt
MEK1
MEK2
CTNNB1 wt
P53
BAX

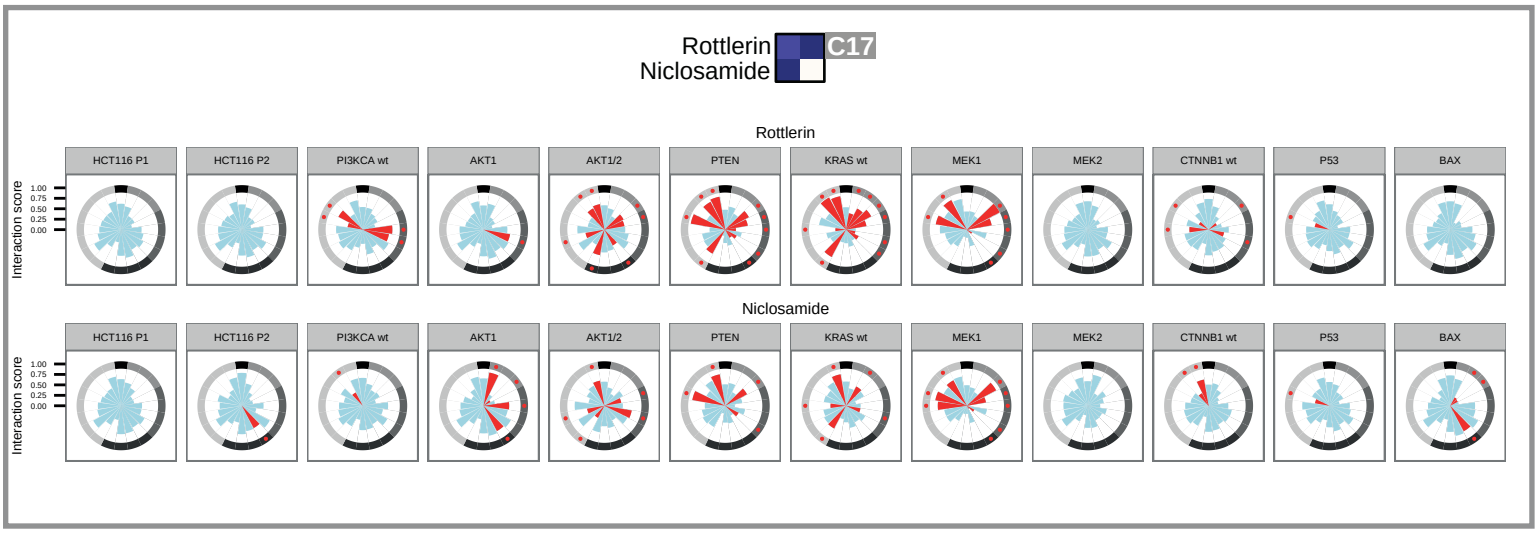

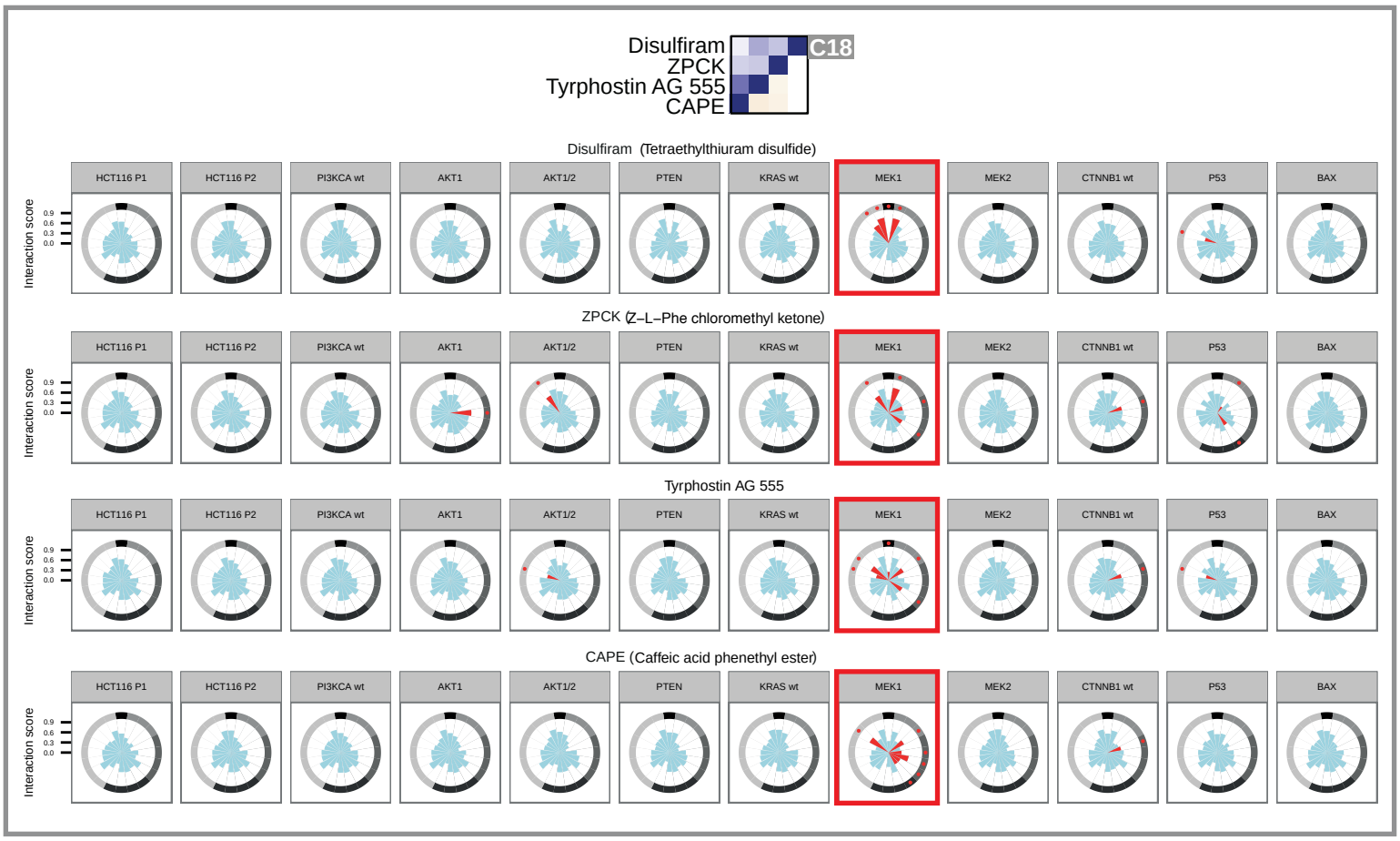

Appendix Figure S9. Association between clustering of compounds as shown in Fig 5A and respective interaction spectra for drugs within clusters.
While in some instances the similarity of drug profiles was a result of coordinated subtle covariation across multiple cell lines and phenotypes, in other cases it was driven by the similarity of distinctive phenotypes of individual cell lines.
For example, the CK2 inhibitors DMAT and TBBz (cluster C5) affected nuclear shape features specifically in cells with only the wildtype copy of PI3KCA (HCT116 PI3KCA wt +/ mt -).
The clustering of the compounds ARP101 and YC-1 in C15 was driven by their distinct phenotypes in cells with only the wildtype copies of CTNNB1 (HCT116 CTNNB1 wt +/ mt -) and PI3KCA (HCT116 PI3KCA wt +/ mt -).
The clustering of compounds in C18 was driven by distinctive interactions with MEK1 KO cells.

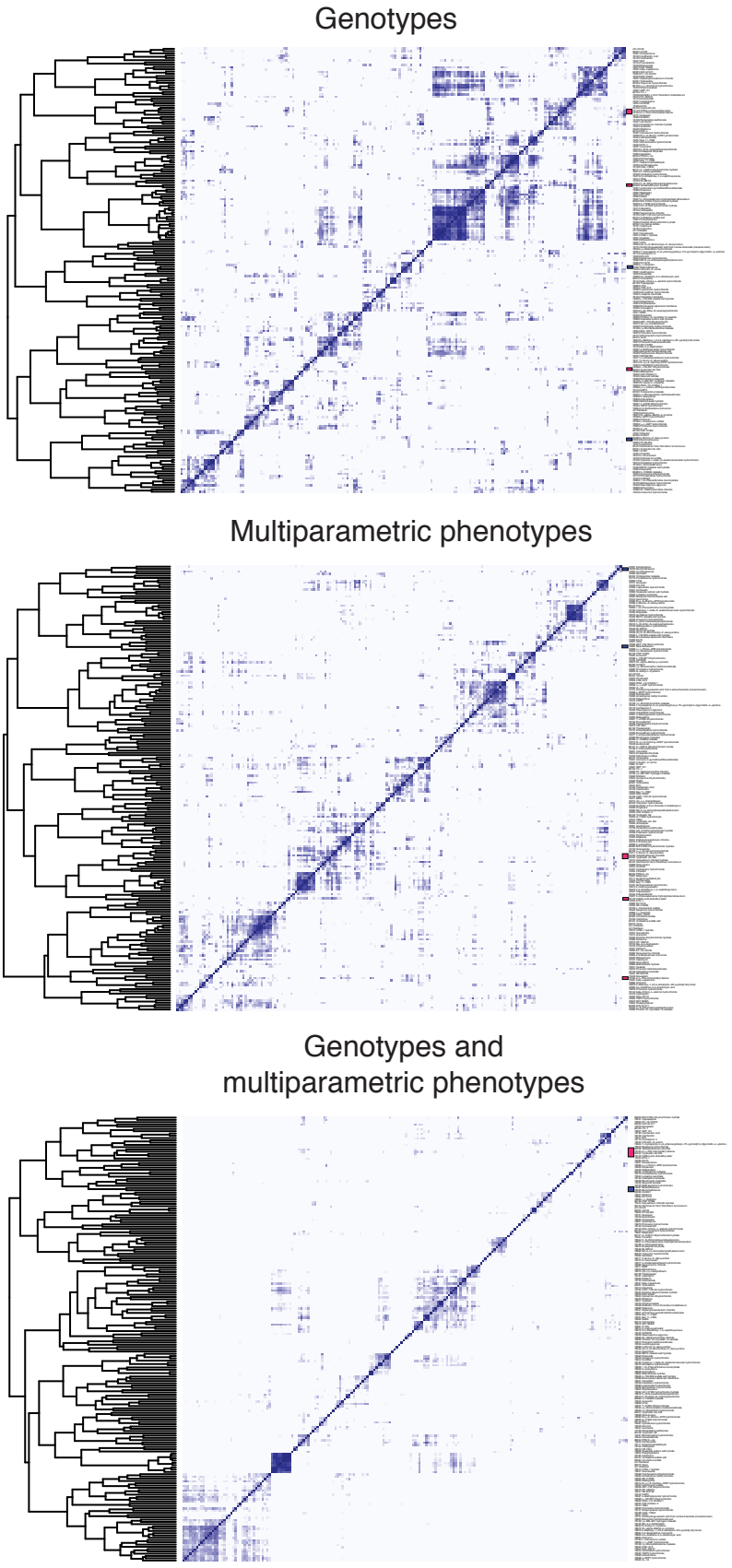

Appendix Figure S10. Integration of phenotypic profiling and chemical-genetic interaction mapping improves resolution.
Unsupervised clustering based on profile correlation using data only on cell number for all twelve genetic backgrounds screened (Genotype), using data from image-based phenotypes of one genetic background (parental HCT116; P2) (Multiparametric phenotypes), or using interaction profiles derived from both genetic backgrounds and image-based phenotypes (Genotypes and multiparametric phenotypes). Each heatmap is ordered based on individual clustering of respective datasets. Blue squares indicate compounds in cluster C4, red squares indicate compounds in cluster C18 (see Fig 5A). In contrast to the low-resolution obtained for genotype or multiparametric phenotype analysis, the combination of phenotypic profiling with chemical-genetic interaction mapping provides distinct high-resolution clusters.

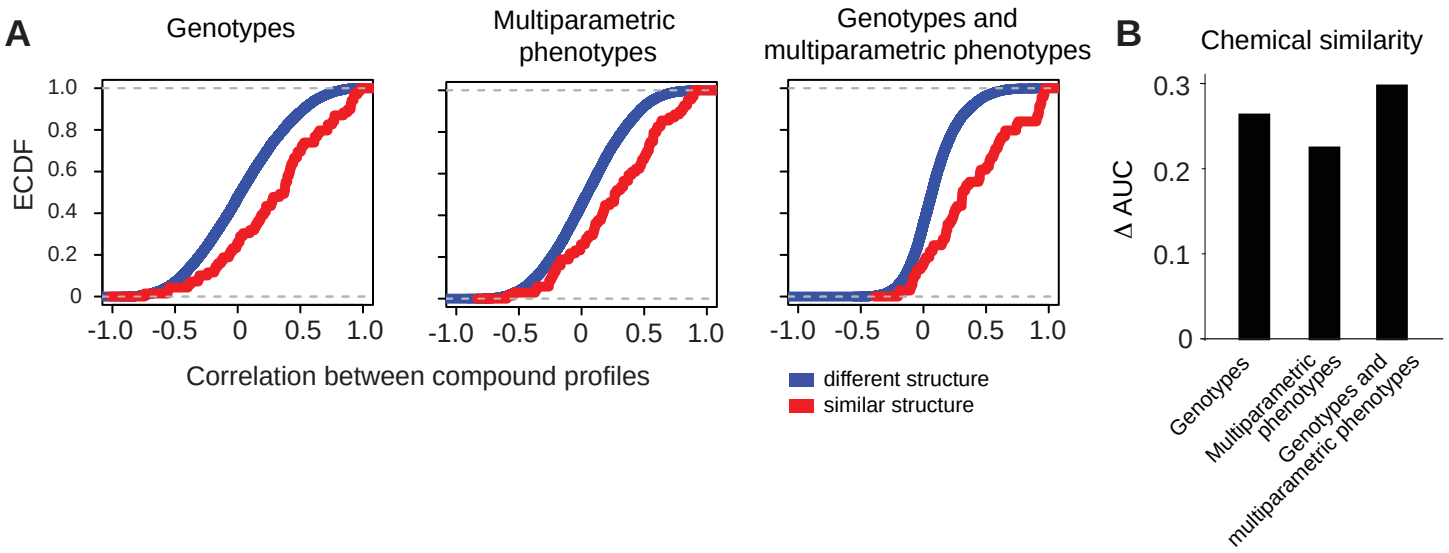

Appendix Figure S11. Image-based chemical-genetic interaction analyses outperforms other methods.
A Compounds that share chemical similarity have a higher correlation of interaction profiles as compared to drugs that do not share chemical similarity, as indicated by the shift of the empirical cumulative density function (ECDF) for shared structures (red curve) compared to non-shared structures (blue curve). Genotype: data only on cell number using 12 genetic backgrounds; Multiparametric phenotypes: data using image-based phenotypes of one genetic background (parental HCT116; P2);
Genotypes and multiparametric phenotypes: interaction profiles derived from both genetic backgrounds and image-based phenotypes.
B Resolution index (Δ AUC) which displays the performance with which each strategy separated drugs that share/do not chemical similarity is shown for aforementioned approaches (see methods for details).

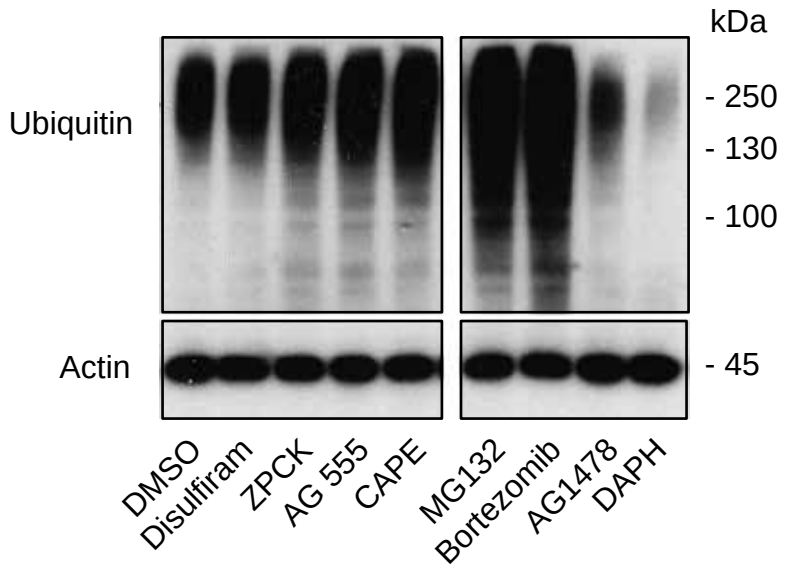

Appendix Figure S12. The EGFR inhibitor tyrphostin AG555 impairs proteasome function. Tyrphostin AG555 increases Ubiquitin abundance. Western blots of total ubiquitin levels after 24 h treatment with compounds at a concentration of 5 µM in HCT116 cells. Tyrphostin AG555 increases the abundance of Ubiquitin, which indicates proteasome inhibition. The proteasome inhibitors MG132 and bortezomib served as positive controls. EGFR inhibitors AG1478 and DAPH did not increase the abundance of ubiquitin. Representative example of 4 independent experiments is shown.